Journal of Materials Chemistry A

ROYAL SOCIETY OF CHEMISTRY

REVIEW

View Article Online
View Journal | View Issue

Cite this: J. Mater. Chem. A, 2023, 11, 3753

Cyano-capped molecules: versatile organic materials

Hongyang Wang, †[a] Chipeng Zhao, †[a] Zuzana Burešová, [b] Filip Bureš *[bc] and Jialei Liu *[a]

Conjugated small molecules bearing the cyano group were reviewed. These organic compounds are extensively used as active layers of solar cells and light-emitting diodes as well as materials with high second- and third-order nonlinearities. Typical organic light conversion agents are also based on CN-capped π-conjugated scaffolds that, in addition, are also increasingly popular for building various organic sensors and probes. More recently, cyanoarenes and dicyanopyrazines were identified as efficient photoredox catalysts. Fundamental structure–property relationships of CN-capped molecules used across the aforementioned areas were elucidated and discussed. The cyano group possessing electron-withdrawing character and linear arrangement is capable of significantly altering electronic and optical properties, and supramolecular arrangement. Hence, extensive property tuning/regulation through the CN group has been demonstrated.

Received 13th December 2022
Accepted 18th January 2023

DOI: 10.1039/d2ta09699d

rsc.li/materials-a

Cyano group as a part of small conjugated molecules

The cyano (C≡N) group bearing both C and N atoms in sp-hybridization is a popular substituent considered a powerful electron-withdrawing moiety with high substituent constants (Hammett $\sigma_p = 0.66$; Pytela $\sigma^i = 0.525$).[1] The cyano group possesses negative inductive and mesomeric effects, and the C≡N bond is highly polarized, which is sensitively reflected by its characteristic stretching vibration in the infrared spectra (~2200 cm^{-1}). Hence, the CN group is tremendously used as a linearly-arranged electron acceptor capable of (i) polarizing π-

[a]Key Laboratory of Prevention and Control of Residual Pollution in Agricultural Film, Ministry of Agriculture and Rural, Institute of Environment and Sustainable Development in Agriculture, Chinese Academy of Agricultural Sciences, Beijing 100081, China. E-mail: liujialei@mail.ipc.ac.cn

[b]Institute of Organic Chemistry and Technology, Faculty of Chemical Technology, University of Pardubice, Studentská 573, Pardubice, 53210, Czech Republic. E-mail: Filip.Bures@upce.cz

[c]Institute of Technology and Business in České Budějovice, Okružní 517/10, České Budějovice, 37001, Czech Republic

† The two authors contributed equally to this work.

Hongyang Wang received his B.S. degree in 2017 and M.S. degree in 2021 from the Hebei Normal University of Science & Technology. Currently, he is pursuing a PhD degree under the supervision of Prof. Jialei Liu at the Chinese Academy of Agricultural Sciences (CAAS), Beijing, China. His research interests include the synthesis of specifically functionalized luminescence materials and their application in green agriculture. He is conducting research on new foliar light fertilizers and light conversion agents for agricultural films.

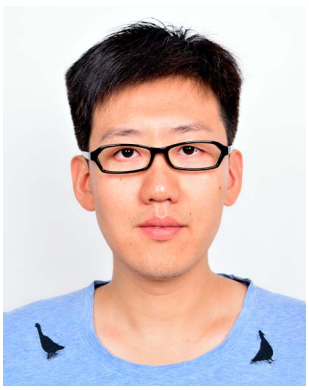

Chipeng Zhao received his M.S. degree from the Chinese Academy of Agricultural Sciences (CAAS) in 2022. From 2019 to 2022, he conducted his graduate study under the supervision of Prof. Jialei Liu. His research interests involve the synthesis and application of versatile organic light conversion agents in agriculture.

conjugated systems, (ii) imparting intramolecular charge-transfer (ICT) when interconnected to an electron donor, (iii) creating an electron rich part of the molecule (due to −I/M effects), (iv) reducing the LUMO level without altering the HOMO, (v) narrowing the HOMO–LUMO gap, (vi) red-shifting the longest-wavelength absorption maxima, (vii) providing a coordination site for cations and electrophiles (*via* nitrogen's lone pair), while (viii) the carbon is prone to a nucleophilic attack.[2] These fundamental properties impart organic CN-functionalized semiconductors various exploitable features such as red-shifted/wide absorption, intense and narrow luminescence, charge-transfer (CT) excited states with reduced energy, low energy losses during CT, reduced electron trapping effect, increased charge-mobility, *etc.*[3–6] Hence, cyano-capped compounds find wide applications across organic electronics and related areas, including organic solar cells (OSCs), organic light-emitting diodes (OLEDs), nonlinear optics (NLO), light conversion agents, organic fluorescent probes, and photoredox catalysis (Scheme 1). Fundamental structure–property relationships of CN-capped organic materials used across these application areas will be discussed. The review does not intend to exhaustively summarize all recent contributions but rather demonstrate the property tuning on suitable examples.

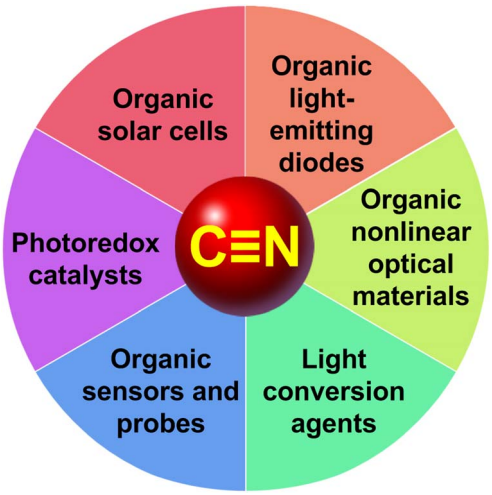

Scheme 1 The main application areas of CN-capped organic molecules covered in this review.

Zuzana Burešová studied organic chemistry at the University of Pardubice, where she finished her master's and doctoral studies in 2016 and 2019, respectively. In 2018, she pursued a three-month internship at the FAU (Erlangen, Germany) under the guidance of Prof. M. Kivala. Her current research activities focus mainly on the design and synthesis of organic π-systems and visible light-initiated organic transformations via photoredox catalysis.

Filip Bureš finished his master's and doctoral studies in organic chemistry at the University of Pardubice in 2002 and 2005, respectively. Subsequently, he pursued studies at the LMU (Germany) and a 14 months postdoctoral fellowship at the ETH Zürich (Switzerland) under the guidance of Prof. P. Knochel and Prof. F. Diederich. After his return to Pardubice, he was habilitated in 2010 and has subsequently been a full professor since December 2017. His current scientific interest includes advanced organic and organometallic materials with manifold applications.

Organic solar cells

In view of the current worldwide situation, energy seems to be a very critical issue. Nowadays, about 85% of the energy is produced from fossil fuels, whereas tidal, wind, biomass, hydroelectric, and solar energy harvesting have undergone rapid development.[7–9] Despite their lower efficiency as compared to inorganic counterparts, organic solar cells (OSCs) represent an alternative technology with reduced material costs/environmental pollution and facilitated manufacturing process.[10,11] In principle, organic photovoltaic cells are capable of converting photons into electrons and supplying electricity

Dr. Jialei Liu is an experienced researcher with a history of research in the field of organic chemistry and optical materials. He is skilled in organic synthesis, functional films, and optical modulation. He has focused on extensive fields of nonlinear optical materials, biodegradable plastic films, and natural products. He obtained his PhD degree (2010) in organic chemistry from the University of Chinese Academy of Sciences, Beijing, China. He is now working as a Professor at the Institute of Environment and Sustainable Development in Agriculture, Chinese Academy of Agricultural Sciences. So far, he has published more than 100 SCI academic peer-reviewed papers.

due to an active organic layer. The used organic π-conjugated materials are generally lightweight, low-cost, flexible, and can be easily adjusted to absorb in the Vis region (HOMO–LUMO gap tuning).[2,12–16] Bulk heterojunction (BHJ) solar cells utilizing a polymeric donor and a fullerene acceptor have been the main research focus in the recent period.[17–22] Fullerene acceptors possess extraordinary charge transport but also low absorption coefficient, difficult purification, and limited property tuning. Hence, non-fullerene acceptors (NFAs) are currently a rapidly growing area of research with very promising preliminary results, reaching power conversion efficiency (PCE) of up to 19%.[23–28] Small conjugated molecules that are easy to synthesize and purify at a low cost, possessing tunable HOMO–LUMO gap and high molar extinction coefficient, are a potential substitute for fullerene acceptors. These organic semiconductors containing CN group(s) will be the main focus of this review.

The simplest cyano-capped semiconductors used in OSCs possess a terminal cyano group appended in a conjugated position, acting as an electron acceptor. These push–pull molecules showed pronounced optical properties and charge mobilities. For instance, Ie *et al.* designed a series of simple π-conjugated compounds **1a–e** based on CN-substituted benzothiadiazole interconnected to variously *N*-substituted phthalimide moieties (Fig. 1, Table 1). It has been shown that a combination of electron-deficient aromatic cycle and CN group leads to a low-lying LUMO level, which is essential for photovoltaic application.[29] Shibata *et al.* synthesized two benzothiadiazole-derived *n*-type materials **2a,b** (Fig. 1) with two terminal CN or CF_3 groups. Both derivatives were utilized in organic photovoltaics, whereas the performance of a device based on cyano-capped **2a** was significantly enhanced. Derivative **2a** bearing two CN groups showed improved crystallinity and diminished carrier recombination and resistance.[30]

Sharma *et al.* prepared a symmetrical perylene bisimide (PBI) derivative **3** with two cyano/nitro-substituted stilbene moieties (Fig. 2). Compared with the devices based on five perylene bisimide derivatives without CN groups as acceptor (they displayed a PCE of 1.92%, 3.11%, 2.54%, 1.54%, and 1.36%, respectively),[31] its electrochemical investigation indicated that a device with a thermally annealed active layer of P3HT:PBI blend possessed an enhanced PCE of 3.17%. Hence, the PBI **3** bearing the CN electron acceptor can effectively improve the PCE by balancing the absorbance and the charge mobility of the blend.[32] Fullerene-free small molecule based on fused acenaphthoisoindoledione **4** (Fig. 2) has been constructed by Zhou *et al.*[33] A blend of **4** as acceptor and P3HT donor provided the PCE up to 1.86% in a solution-processed BHJ solar cell. Therein, the introduction of electron-withdrawing CN group on the fluoranthene-fused imide skeleton effectively tuned its LUMO levels (around −3.5 eV), and optimized the open circuit voltage (V_{oc}) of the photovoltaic devices, making **4** a promising candidate as a new electron acceptor in BHJ photovoltaic cells. Most notably, when the CN group in **4** was substituted for an analogical and simple electron-withdrawing group (a methyl-ester group), a new acceptor was yielded. Its blend with P3HT only exhibited a relatively low PCE of 1.61% in the BHJ solar cells.[34]

Fluorene can be combined with diketopyrrolopyrrole (DPP) units *via* 2,5-thienylene linkers as demonstrated by Li *et al.* in oligomeric **5** (Fig. 2). As compared to previous small cyano-capped molecules **1–4** (Table 1), this designed acceptor possesses red-shifted absorption maxima, significantly reduced HOMO–LUMO gap, deepened LUMO level, and good electron mobility (up to 10^{-3} cm^2 V^{-1} s^{-1}). A BHJ solar cell built on **5** and P3HT showed PCE of 2.37%.[35]

Two geminal cyano groups attached to a π-conjugated backbone *via* olefinic linker is well-known as dicyanovinyl (DCV) moiety.[36] It is a tremendously popular electron acceptor across organic dyes, chromophores, semiconductors, *etc.*,

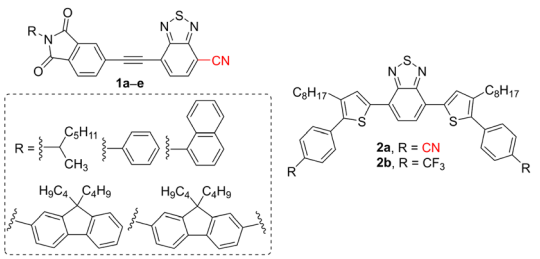

Fig. 1 Small CN-substituted benzothiadiazole derivatives for application in OSCs.

Table 1 Optoelectronic parameters of NFAs **1–5** based on cyano(-hetero)arene/olefin

Acceptor	λ_{max}^{A} (nm eV^{-1})	E_g (eV)	E_{LUMO} (eV)	Donor	PCE (%)	Ref.
1a	*ca.* 375/3.31	2.97	−3.48	P3HT	0.19	29
1b	*ca.* 375/3.31	2.97	−3.47	P3HT	0.12	29
1c	*ca.* 375/3.31	2.98	−3.48	P3HT	—	29
1d	*ca.* 310/4.00	2.95	−3.48	P3HT	0.32	29
1e	*ca.* 315/3.94	2.94	−3.48	P3HT	0.28	29
2a	350/3.54	—	−3.33	P3HT	0.86	30
2b	335/3.70	—	−3.30	P3HT	0.09	30
3	655/1.89	1.72	−3.90	P3HT	3.17	32
4	410/3.02	—	−3.48	P3HT	1.86	33
5	693/1.79	1.66	−3.65	P3HT	2.37	35

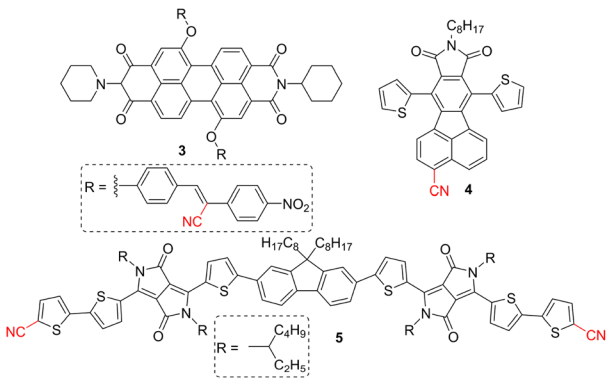

Fig. 2 CN-capped perylene bisimide (**3**), acenaphthoisoindoledione (**4**) and fluorene-DPP-CN (**5**) acceptors for OSCs.

mostly due to its easy introduction *via* Knoevenagel condensation of an aldehyde and malononitrile. As compared to single CN-substituted molecules, DCV-functionalization brings about an enlarged π-system by an additional olefinic linker end-capped by two CN groups. Hence, DCV-substituted compounds possess bathochromically and hyperchromically shifted absorption spectra, an important requirement for photovoltaic devices.[37] Central electron releasing carbazole decorated by two benzothiadiazole acceptors further supported by terminal DCV moieties allowed the construction of $(A–A)_2–D$ derivatives **6** (Fig. 3). Its use as an acceptor along with PCE10 polymeric donor in BHJ solar cell resulted in a device efficiency reaching 5.3%. DCV-capped semiconductor **6** showed low-lying LUMO (Table 2) and efficient ICT, while its rigid-planar structure enhanced intermolecular interactions and pronounced carrier mobilities.[38]

Duan *et al.* reported two analogous perfluorinated oligothiophene derivatives **7a**, **7b** bearing five or seven thiophene rings (Fig. 3). Despite Duan's research being primarily focused on the fluorination effect, two terminal DCV moieties affected the HOMO/LUMO levels of **7** and imparted general electron deficiency. Hence, oligomers **7a**, **7b** were used as NFAs and achieved PCEs of 4.5 and 1.8%, respectively (Table 2).[39]

Dicyanovinyl can be combined with other carbonyl-based acceptors, such as indan-1,3-dione, to gain a strong electron-withdrawing moiety – 1,1-dicyanomethylene-3-indanone (IC). Besides the parent IC, 2-(5,6-difluoro-3-oxo-2,3-dihydro-1*H*-inden-1-ylidene)malononitrile (FIC) is also often employed in semiconductors. These planar acceptors red-shift the absorption maxima, reduce band gap, increase electron deficiency, and enhance photovoltaic performance.[40–42] Triphenylamine (TPA) is very often used to construct star-shaped systems such as **8a**, **8b** (Fig. 4) bearing three IC terminal acceptors and

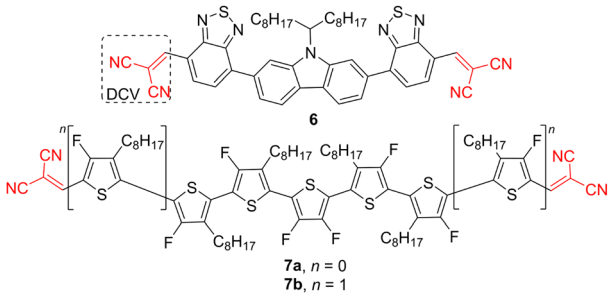

Fig. 3 Two representative examples of DCV-capped semiconductors having $(A–A)_2–D$ (**6**) and oligomeric (**7**) arrangement.

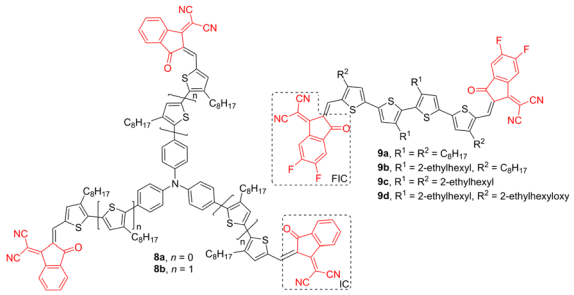

Fig. 4 The molecular structures of TPA (**8**)- and oligothiophene (**9**)-based semiconductors bearing peripheral IC and FIC acceptors.

thiophene/bithiophene linkers. Their LUMO levels (−3.6 eV; Table 3) are well-suited to accept electrons from P3HT donor (−2.8 eV), and the **8a**, **8b**:P3HT blend showed promising performance in flexible organic photovoltaic devices with PCE up to 1.13% (**8a**). Furthermore, **8a** has been reported to promote an efficient charge extraction process while limiting charge recombination at the interface.[43]

In contrast to odd-membered oligothiophenes **7** (Fig. 3), Zhou *et al.* developed tetrathiophene (4T) semiconductors **9a–d** with two FIC acceptors (Fig. 4). Whereas the FICs affect mostly optical properties, R^1 and R^2 substituents along the 4T backbone allowed to effectively tune solubility, packing mode, film morphology, and charge mobility. Derivatives **9a–d** used as acceptors along with PBDB-T/D18 donors afforded PCE up to 12.04% (Table 3).[44]

Subphthalocyanine core decorated with three peripheral (F) IC acceptors (Fig. 5) with PBDB-T donor have been utilized in OSCs by Hang *et al.*, achieving the PCE of 4.69 and 3.80%, respectively.[45] Compounds **10a**, **10b** showed extraordinary broad absorption with the full width at half maximum exceeding 260 nm and narrow optical bandgaps (~1.6 eV; Table 4). When comparing both derivatives, **10b** bearing FIC acceptor possesses deepened LUMO level and higher open-circuit voltage (V_{oc} = 0.81 V). Thiophene and selenophene were utilized as linkers in ladder-type derivatives **11** (Fig. 5) bearing two IC acceptors. A solar cell based on the **11**:J51 blend afforded PCE of 8.6%.[46]

Enlarged seven-ring fused core of indacenodithieno[3,2-*b*]thiophene end-capped with two IC acceptors is known as ITIC **12** (Fig. 6). It showed wide absorption, reduced energies of the frontier molecular orbitals, good *n*-type charge mobility, and miscibility with low band gap polymeric donors such as PTB7-TH as well as suppressed self-aggregation of the central core

Table 2 Optoelectronic parameters of DCV-capped semiconductors **6**, **7**

Acceptor	$\lambda_{max}{}^{A}$ (nm eV^{-1})	E_g (eV)	E_{LUMO} (eV)	Donor	PCE (%)	Ref.
6	517/2.40	2.02	−3.64	PCE10	5.30	38
7a	*ca.* 540/2.30	1.93	−3.48[a]/−1.93[b]	PCE10	4.50	39
7b	*ca.* 555/2.23	1.81	−3.31[a]/−1.76[b]	PCE10	1.80	39

[a] Calculated LUMO levels of **7a** and **7b** with B3LYP/6-31G(d,p). [b] Calculated LUMO levels of **7a** and **7b** with ωB97XD, respectively.

Table 3 (F)IC-capped semiconductors and their fundamental properties

Acceptor	λ_{max}^{A} (nm eV^{-1})	E_g (eV)	E_{LUMO} (eV)	Donor	PCE (%)	Ref.
8a	575/2.16	1.93	−3.60	P3HT	1.13	43
8b	665/1.86	1.71	−3.60	P3HT	0.86	43
9a	704/1.76	1.47	−4.09	PBDB-T	5.53	44
9b	654/1.90	1.54	−4.02	PBDB-T	9.09	44
9c	667/1.86	1.52	−3.98	PBDB-T/D18	10.15/12.04	44
9d	651/1.90	1.60	−3.86	PBDB-T	8.27	44

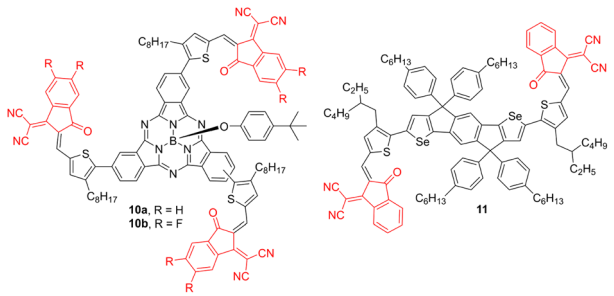

Fig. 5 The molecular structures of subphalocyanine and thiophene-selenophene cores decorated with IC acceptor.

due to a twisted arrangement of the peripheral substituents. A solar cell with **12**:PTB7-TH blended film showed PCE of 6.80% (Table 4).[47]

In order to broaden its light absorption and enhance the photocurrent, the parent ITIC (**12**) has been subjected to various further structural modifications. For example, Lu *et al.* have prepared two new ITICs **13a**, **13b** (Fig. 6) bearing (di)methyl-substituted IC units with slightly increased LUMO levels (Table 4). This relatively minor structural tuning improved the PCE of the OSC using **13a**, **13b**:PBDB-blend up to 12.05/11.29%.[48] Further synthetic attempts (Fig. 6) were directed towards the extension of the π-conjugated core by 2,5-thienylene units (**14**) or introducing hexyl substituents in the position 2 of the appended phenyl rings (**15**), making the whole acceptor more nonplanar. These structural features allowed obtaining OSCs with the PCE around 10% (Table 4).[49–55]

Lin *et al.*[56] reported a new ITIC-inspired molecular acceptor **16** named IDIC (Fig. 6), which strongly absorbs within the region of 500–780 nm, possesses a narrow optical bandgap (1.60 eV), and high electron mobility (1.1×10^{-3} cm^2 V^{-1} s^{-1}). It has been used to construct OSCs along with various (polymeric) donors (namely PDBT-T1, PTFBDT-BZS, PTZ1, and H11) with the PCEs within the range of 8.06–9.73% (Table 4).[56–58]

Indan-1,3-dione (IO) and 1,1-dicyanomethylene-3-indanone (IC) were further utilized as parent scaffolds to study the influence of end groups on NFA's performance (CN *vs.* CO). For instance, Lin *et al.* have compared perylene diimide-fused dithiophenepyrroles with the IO and IC end groups bearing additional fluorine/chlorine atoms. The prepared large A–D–A–D–A acceptors bearing peripheral IC groups afforded significantly enhanced PCE up to 9.0%.[59] Huang *et al.* have extensively varied the IC moiety focusing on fused-ring electron acceptors (FREAs). A large series of ITIC derivatives bearing variously modified IC revealed facile modification of the HOMO/LUMO levels and band gap as well as the realization of higher PCE in organic photovoltaic cells with CN-substituted molecules.[60] In contrast, dichloroindan-1,3-dione IO4Cl, similar to **12** without CN groups (Fig. 6), showed an outstanding PCE of 26.1% as measured under indoor illumination conditions (2700 K LED at 1000 lux).[61] However, a measurement at standard AM 1.5 G conditions revealed diminished PCE = 9.80%. In summary, IC-terminated NAFs may benefit from higher absorption coefficients, tailored HOMO/LUMO levels/band gaps, lower energy loss, and effective charge transfer.

Dicyano rhodanine (mostly *N*-substituted) is another widely used electron-withdrawing moiety with two geminal cyano groups (DCV) and easy synthesis. As compared to the parent rhodamine, dicyanorhodanine imparts higher ICT and makes the π-conjugated system more electron deficient. Furthermore, the dicyanorhodanine-based semiconductors show small crystal domain size, uniform morphology, and smoother blend film surface, which is advantageous for efficient charge

Table 4 Optoelectronic parameters of semiconductors bearing the IC acceptors

Acceptor	λ_{max}^{A} (nm eV^{-1})	E_g (eV)	E_{LUMO} (eV)	Donor	PCE (%)	Ref.
10a	629/1.97	1.68	−3.90	PBDB-T	4.69	45
10b	634/1.96	1.66	−4.06	PBDB-T	3.80	45
11	*ca.* 740/1.68	1.52	−3.79	J51	8.60	46
12	702/1.77	1.59	−3.83	PTB7-TH	6.80	47
13a	700/1.77	1.60	−3.98	PBDB-T	12.05	48
13b	692/1.79	1.63	−3.93	PBDB-T	11.29	48
14	*ca.* 740/1.68	1.46	−3.82	PBDB-T1	9.12	51
15	*ca.* 700/1.77	1.58	−3.82	J61	10.57	52
16	722/1.72	1.60	−3.91	See text	8.06–9.73	56–58

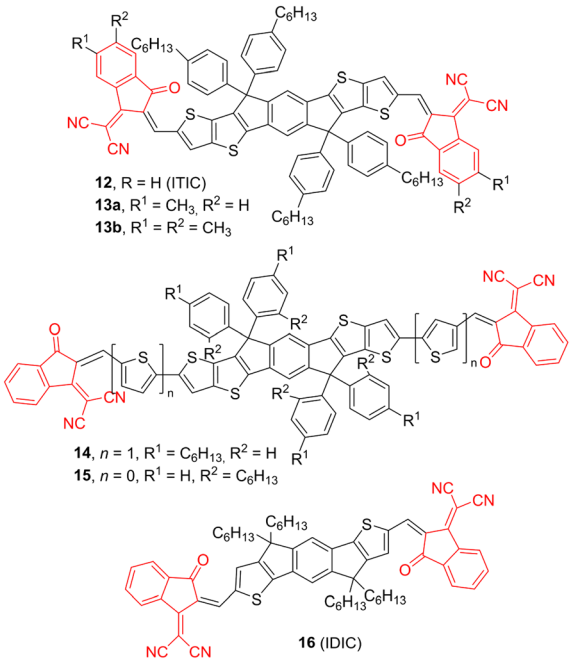

Fig. 6 ITIC family of small acceptors for OSCs.

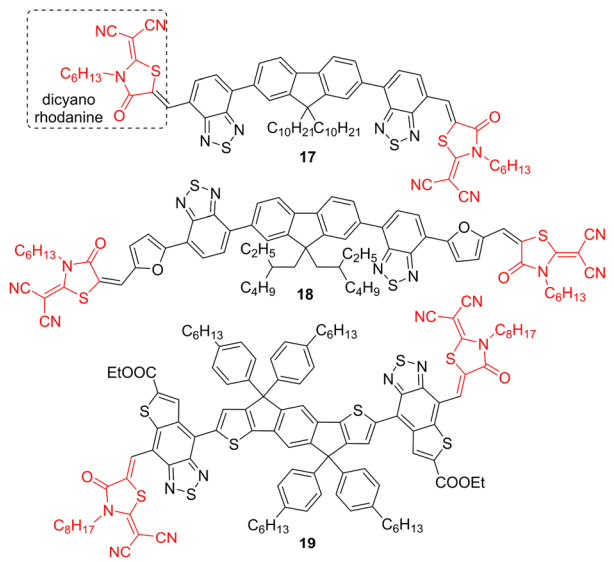

Fig. 7 Dicyano rhodamine derived molecular acceptors.

transport and improved efficiency of organic photovoltaic devices.[37] For instance, a quadrupolar system **17** (Fig. 7) based on a fluorene core, two benzothiadiazole linkers, and two peripheral dicyanorhodanines was investigated.[62] It showed pronounced absorption and lowered LUMO energy, and its blend with polymeric donor (PffBT4T-2OD) afforded the OSC with the PCE of 8.4%, FF of 70.7%, and external quantum efficiency (EQE) of 84% (Table 5). The π-conjugated backbone of **17** has further been extended by two furan units, as shown for **18**. Its film with PTB7-Th polymeric donor has been used in OSC with an improved PCE of 10.7%.[63] IDT core, similar to **16**, flanked by two thiophene-fused benzothiadiazole units and terminal dicyanorhodanines was used as molecular acceptor **19** by Xu *et al.* (Fig. 7).[64] This derivative possesses a reduced band gap (1.92 eV) because of efficient ICT between the dicyanorhodamine and the central auxiliary thiophene donors, and its photovoltaic performance with PTB7-Th donor reached 9.07% (PCE) and short circuit current density (J_{sc}) over 20.33 mA cm^{-2}.

Organic light-emitting diodes

The recent rapid development of organic electronics is also due to remarkable progress in the design, preparation, and understanding of organic light-emitting semiconductors. Organic semiconducting materials possess a variety of advantageous properties, including low density, easy and inexpensive preparation and structural tuning and solution processibility that were successfully utilized in organic solid-state lasers,[65] organic light-emitting diodes (OLED),[66] organic field-effect transistors,[67] smart materials,[68] biological imaging,[69] biochemical sensing[70] and many others. Since the first OLED reported by Kodak in 1987,[71] this sandwich technology has evolved into commercially very successful and popular devices. The OLED utilizes the principle of electroluminescence – a radiative recombination of electrons and holes in a semiconducting material, releasing the excess of energy as photons. The organic materials used in OLEDs involve hole/electron-injection/transport layers, electron/hole-blocking layers, and most importantly, organic emitting layers. According to the exciton harvesting mechanism, the current organic emitters can be divided into three main generations, including fluorescent, phosphorescent, and thermally-activated delayed fluorophores (TADF).[72] CN-substituted small-molecules with D–A arrangement and their TADF properties were reviewed by Cao *et al.*[73] Mono/multicyano-substituted benzenes, mono/dicyano-derived aromatic *N*-heterocycles, and acrylonitriles were covered, and their structure–property relationships were systematically discussed. This work provides an important reference and guidance for the current development of TADF materials containing CN group(s) and their manifold applications. A typical organic emitter consists of a π-conjugated backbone functionalized with both electron-withdrawing/releasing substituents and moieties,

Table 5 Optoelectronic parameters of dicyano rhodanine derivatives **17–19**

Acceptor	$\lambda_{max}{}^{A}$ (nm eV^{-1})	E_g (eV)	LUMO (eV)	Donor	PCE (%)	Ref.
17	498/2.49	2.16	−3.55	PffBT4T-2OD	8.40	62
18	522/2.38	2.07	−3.81	PTB7-TH	10.70	63
19	770/1.61	1.92	−3.78	PTB7-TH	9.07	64

allowing precise color-tuning. In this respect, the cyano group proved to be a very useful linear acceptor. *N*,*N*-Diphenylamino and stilbene moieties are very common structural features of OLED's fluorescent materials, *e.g.*, see derivative **20** in Fig. 8. This CN-functionalized red-emitting dye has been revealed as a bipolar material allowing efficient charge injection/transport as well as recombination. A double-layered OLED using **20** showed a luminance of 3290 cd m^{-2} at the current density of 100 mA cm^{-2} and EQE of 1.1%.[74] A very similar quadrupolar (D–π–)$_2$A derivative **21** based on central dicyanonaphthalene core has been investigated by Hung *et al.*[75] An OLED based solely on **21** displayed luminous efficiency of 2.8 cd A^{-1} and EQE of 0.80%. Biphenylene scaffold **22** decorated by *N*,*N*-diphenylamino donor and phenanthroimidazole acceptor has been investigated by Zhang *et al.*[76] The imidazole has been further *N*-substituted by 4-cyanophenyl moiety, which significantly improved EQE up to 7.8% (Table 6) by modulating the emissive state. The OLED based on **22** showed luminous efficiency of 10.5 cd A^{-1} and emitted light with the CIE coordinates (0.16, 0.16) corresponding to a pure blue. Anthracene is another prominent π-conjugated scaffold used in the construction of fluorophores. D–π–A derivative **23** (Fig. 8) utilizing methoxy donor and cyano acceptor showed the highest luminous efficiency (6.1 cd A^{-1} at 2 mA cm^{-1}) across related derivatives. Moreover, the CIE coordinates (0.15, 0.06; Table 6) of **23** match well with the HDTV standard blue.[77] Spiro compounds are another popular group of sterically demanding emitters, and derivative **24** combining benzanthrone and fluorene moieties and two peripheral CN groups is a typical example. It has been shown that its LUMO occupies both the central π-system and the cyanophenyl moieties, and **24** possesses CT character. The OLED based on **24** showed luminous efficiency of 10.3 cd A^{-1} and an EQE of 10.2% at a constant luminance of 1000 cd m^{-2}. Compound **24** is a highly efficient deep blue emitter with the CIE coordinates (0.14, 0.11).[78] DCV moiety is less employed in organic emitters as compared to single-CN derivatives; cyclohexane- and pyran-4-one-derived compounds **25** and **26** represent rather simple push–pull molecules.[79,80] For instance, an OLED device built on **26** showed luminous efficiency of 4.4 cd A^{-1} and CIE coordinates (0.65, 0.35) (Table 6).

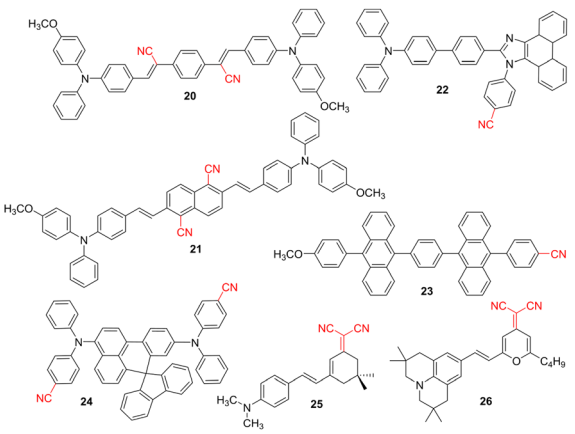

Fig. 8 The molecular structure of representative CN-substituted OLED materials.

Organic nonlinear-optical materials

Since the discovery of laser in 1960, various nonlinear optical (NLO) phenomena, such as second/third-harmonic generation, two-photon absorption, amplification, scattering, conversion, oscillation, modulation, *etc.*, have been experimentally observed.[81–95] Along with these fundamental discoveries, the NLO community also became very interested in organic materials with pronounced NLO activity both at the molecular and supramolecular levels.[96,97] It has been realized shortly that traditional inorganic crystalline materials can be completed/substituted by organic molecules with distinct properties such as flexibility, facile property tuning, solution processability, and inexpensive preparation. A general drawback of organic molecules is their centrosymmetric supramolecular arrangement, which, however, can be suppressed by proper structural tuning.[2,98,99] Due to its negative mesomeric effect, the CN group shows strong D–A interaction if interconnected to an electron-donor *via* a π-conjugated system (D–π–A system). Hence, CN-capped push–pull chromophores have been tremendously investigated as active NLOphores. D–π–A arrangement brings pronounced ICT, dipolar character, and red-shifted absorption – fundamental aspects of an NLO active substance. The current trends in developing new NLO-active organic molecules involve multichromophoric compounds having extraordinary arrangements inspired by the alphabet.[100] Hence, various H-, L-, T-, V-, X-, and Y-shaped NLOphores were developed to date. The most popular tripodal Y-shaped molecules can be built either on imidazole[101] or triphenylamine (TPA) cores terminated by three acceptors. For instance, we have decorated TPA core by

Table 6 Fundamental parameters of CN-capped OLED materials **20–26**

Emitter	λ_{max}^{A} (nm eV^{-1})	λ_{max}^{E} (nm eV^{-1})	$CIE_{x,y}$	EQE (%)	Ref.
20	—	598/2.07	—	1.10	74
21	507/2.45	630/1.97	(0.63, 0.37)	0.80	75
22	ca. 360/3.44	445/2.79	(0.16, 0.16)	7.80	76
23	405/3.06	452/2.74	(0.15, 0.06)	12.00	77
24	400/3.10	450/2.76	(0.14, 0.11)	10.20	78
25	500/2.48	650/1.91	—	—	79
26	520/2.38	615/2.02	(0.65, 0.35)	—	80

Table 7 Fundamental properties of CN-capped TPA chromophores **27a–l**[102]

NLOphore	$\lambda_{max}{}^{A}$ [a] (nm eV^{-1})	$\lambda_{max}{}^{E}$ [b] (nm eV^{-1})	Φ^{F} [c] (%)	HOMO–LUMO[d] gap (eV)	δ_{2PA}[e] (GM)
27a	339/3.66	377/3.29	0.62	3.50	—
27b	394/3.15	460/2.70	0.48	2.86	260 (770)
27c	372/3.33	448/2.77	0.64	3.04	566 (760)
27d	387/3.20	458/2.71	0.59	2.89	785 (780)
27e	403/3.08	510/2.43	0.51	2.65	1100 (810)
27f	453/2.74	549/2.26	0.29	—	757 (830)
27g	470/2.64	611/2.03	0.29	—	667 (810)
27h	413/3.00	497/2.49	0.59	2.63	620 (810)
27i	420/2.95	533/2.33	0.69	2.71	852 (810)
27j	414/3.00	499/2.48	0.55	2.59	631 (810)
27k	397/3.12	475/2.61	0.46	2.54	148 (750)
27l	412/3.01	516/2.40	0.49	2.58	375 (830)

[a] The longest-wavelength absorption maxima measured in THF. [b] The emission maxima measured in THF. [c] Fluorescence quantum yield in THF. [d] The electrochemically determined HOMO–LUMO gap in acetonitrile. [e] Two-photo absorption cross-section (the wavelength of the maximum 2 PA cross-section is shown in parenthesis).

systematically evaluated CN-acceptors to tailor absorption/emissive maxima, HOMO–LUMO gap, two-photon absorption cross-section as well as thermal robustness (Table 7).[102] Hence, tripodal Y-shaped molecules **27a–l** (Fig. 9) bearing peripheral single CN-substituted, dicyanovinyl, and dicyanobenzene/imidazole/thiophene moieties and varied π-linkers proved to be tunable NLOphores allowing elucidation of fundamental structure–property relationships. 4-Cyanostyryl (**e**) and 2,6-dicyanophenylethynyl (**i**) units turned out to be the most efficient peripheral acceptors in terms of the achieved two-photon absorption cross-sections.

Dicyanoimidazole (DCI), dicyanobenzene (DCB), and dicyanopyrazine (DCP) are other popular aromatic (hetero) cyclic electron-withdrawing moieties of NLO active compounds **28–30**. DCI has been used in the construction of Y-shaped imidazoles **28** bearing various electron donors D such as methoxy, *N*,*N*-dimethylamino or ferrocenyl and systematically enlarged π-linker.[103–107] These structural changes allowed to shift the longest-wavelength absorption maxima by up to 70 nm, narrowed the HOMO–LUMO gap by more than 1.1 eV, and tuned the second-order NLO response within the range of 19–40 × 10^{-30} esu as measured by hyper-Rayleigh scattering at 1064 in dichloromethane. Isolobal X-shaped derivatives **29** and **30** were built on DCB/DCP cores by attaching various π-linkers, which tuned their optical and electrochemical gaps within the range of 335–458/354–499 nm and 2.54–1.87/2.26–1.50 eV, respectively.[108,109] The measured second-order polarizabilities β were generally larger for pyrazines but the effect of stronger acceptor diminishes with gradual π-linker extension.

2-(3-Cyano-4,5,5-trimethylfuran-2(5*H*)-ylidene)malononitrile (TCF) is another very powerful and popular acceptor combining three CN groups. It has been utilized in representative Y-shaped TPA chromophores **31a**, **31b** (Fig. 11). Further property tuning has been achieved by furan or thiophene linkers, and both chromophores showed absorption within the region of 610–630 nm, good optical nonlinearity, and thermal stability (Table 8).[110]

Yang *et al.* designed a series of linear push–pull molecules **32** with either bridged diaminophenothiazine-π-TCF (**a**/**c**) or diaminophenyl-π-TCF (**b**/**d**) arrangement (Fig. 11). It has been revealed that how the bridging and extension of the π-system affect absorption maxima, NLO and thermal properties (Table 8). Based on these findings, derivatives **32a–d** proved to be promising high-performance organic electro-optic and photorefractive

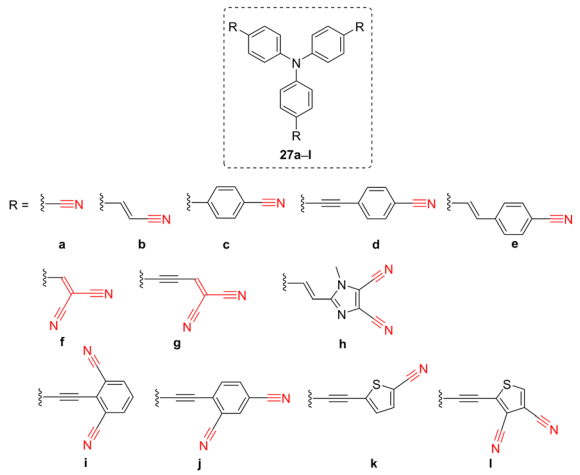

Fig. 9 Property tuning in CN-capped tripodal NLOphores based on triphenylamine.

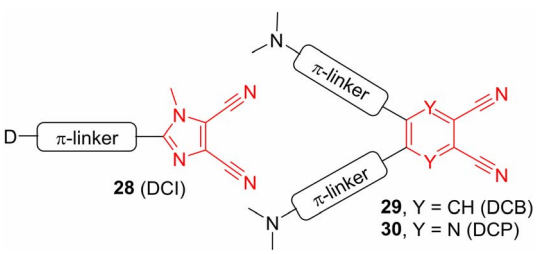

Fig. 10 Dicyanoimidazole, dicyanobenzene and dicyanopyrazine-derived Y- and X-shaped chromophores.

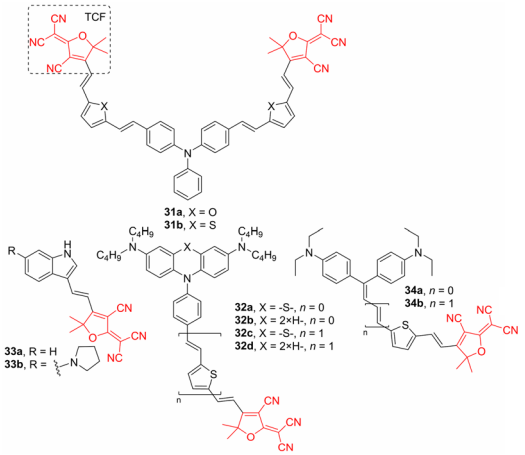

Fig. 11 Representative TCF-functionalized NLOphores.

materials.[111] TCF is also a very popular acceptor unit of small indole-derived push–pull molecules such as **33a, 33b.** It has been shown that further substitution of the indole by pyrrolidine donor red-shifts the absorption maxima and drastically enhances the second-order NLO response (Table 8) as well as increases charge mobility.[112] Yang *et al.* interconnected Michler's ketone moiety to TCF to gain simple push–pull chromophores **34a, 34b** (Fig. 11). Along with planar and polarizable olefinic/2,5-thienylene π-backbone; these chromophores possess enhanced macroscopic electro-optic coefficients (Table 8).[113]

TCF-functionalized molecules were used to construct anionic polymethine salts **35a–c** (Fig. 12) bearing phosphonium counterions.[114] Whereas (non)linear optical properties of mono- and dicationic compounds **35a, 35b** were strongly dependent on the concentration (due to aggregation), hexacationic complex **35c** significantly resisted intermolecular interaction at higher concentrations. Its macroscopic third-order nonlinearity measured by the Z-scan technique (1.55 μm) in the neat film is 3.6×10^{-11} esu, which is larger than that measured for **35a, 35b**

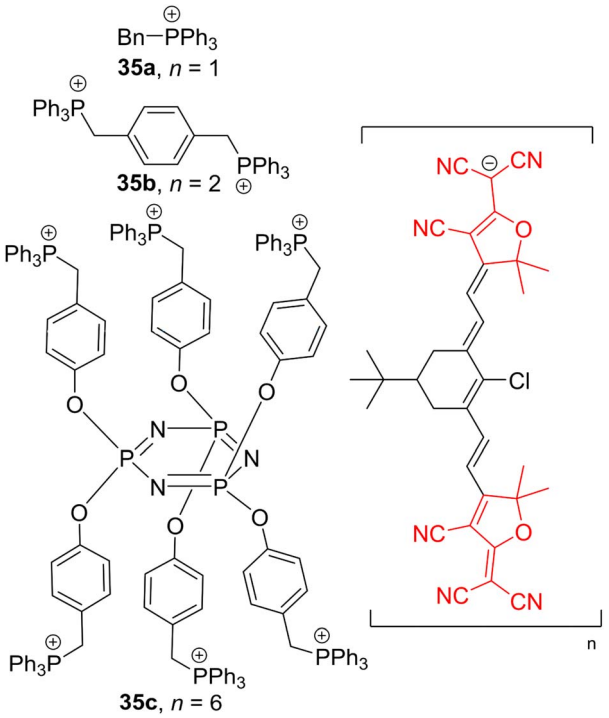

Fig. 12 Chemical structure of anionic TCF-polymethine salts **35a–c**, including the corresponding phosphonium cations.

(2.3 and 3.4 × 10^{-11} esu). Hence, a strong intramolecular anion–cation interaction in **35c** provides a steric repulsive effect diminishing intermolecular interactions, which results in an efficient translation between the microscopic and macroscopic polarizabilities.

Light conversion agents

CN-capped molecules can also be utilized as light conversion agents that are especially useful to convert unproductive yellow-

Table 8 Fundamental properties of NLOphores **31–34**

NLOphore	$\lambda_{max}{}^{A}$ (nm eV^{-1})	HOMO–LUMO gap (eV)	β_{max}/(10^{-30} esu)	$r_{33}{}^{g}$/(pm V^{-1})	Ref.
31a	621[a]/2.00	—	1023.00[c]	—	110
31b	618[a]/2.01	—	1091.00[c]	—	110
32a	599[a]/2.07	2.39	329.90[d]	31.00	111
32b	659[a]/1.88	2.17	458.87[d]	47.00	111
32c	659[a]/1.88	1.86	962.94[d]	72.00	111
32d	730[a]/1.70	1.68	1561.80[d]	95.00	111
33a	309[b]/4.01	—	106.40[e]	10.60	112
33b	550[b]/2.25	—	798.80[e]	23.50	112
34a	725[a]/1.71	1.963	713.00[f]	149.00	113
34b	750[a]/1.65	1.766	995.00[f]	143.00	113

[a] $\lambda_{max}{}^{A}$ was measured in $CHCl_3$. [b] $\lambda_{max}{}^{A}$ was measured in the solution of THF. [c] β values were measured by Hyper-Rayleigh Scattering technique in $CHCl_3$ using the fundamental excitation wavelength of 1064 nm. [d] β values were calculated using Gaussian 09 at the CAM-B3LYP/6-31+G* level and the direction of the maximum value is directed along the charge transfer axis of the chromophores. [e] The β components were calculated using Gaussian 09 and dynamic (at the 1310 nm) average β values were measured. [f] β values were calculated using Gaussian 03 at the B3LYP/6-31 g(d) level and the direction of the maximum value is directed along the charge transfer axis of the chromophores. [g] r_{33} values were measured at a wavelength of 1310 nm.

green (510–580 nm) and ultraviolet light (280–380 nm) into red-orange (600–700 nm) and blue-violet light (400–480 nm) that are essential wavelengths for photosynthesis. There are three types of light conversion agents,[115–122] including (i) rare-earth sulfides, (ii) rare-earth complexes bearing organic ligands (mostly Eu^{3+} and Sm^{3+} complexes), and (iii) pure organic fluorescent dyes. Rare-earth sulfides possess very good stability, but they also tend to deliquescence and disperse, and their fabrication requires high-temperature sintering. Rare-earth complexes possess stronger fluorescence and generally better compatibility with a polymer matrix, but these complexes fail to convert yellow-green into red-orange light. In principle, organic fluorescent dyes are well-soluble in organic resins and possess fluorescence emission bands easily adjustable to an absorption spectrum of different crops. Hence, inexpensive and easy-to-obtain agricultural films can be produced. The organic dye used as a light conversion agent should possess pronounced emissive properties and high fluorescence quantum yield along with none or minor quenching upon increasing its concentration/embedding in a matrix. The organic dye should also withstand long-term exposure to solar radiation and not undergo degradation and oxidation. Moreover, molecular optical properties measured in a solution are often not fully mirrored in a polymeric matrix, which may also result from diminished mechanical and chemical stability upon doping with the selected light conversion agent. Aggregation-induced emission (AIE) and TADF were utilized as two leading mechanisms in the design of organic light conversion agents.[123] Variety of π-conjugated organic scaffolds were already examined, with triphenylacrylonitrile proving to be a benchmark compound. For instance, Wang *et al.* have optimized the parent triphenylacrylonitrile backbone by attaching additional aryls at positions 3 and 4 leading to derivatives **36a–e** (Fig. 13). These highly efficient blue-violet light conversion agents, biphenyl derivative **36e** in particular, exhibited crystallization-induced emission accompanied by a strong fluorescence (Φ^F of 0.833 and 0.107 in the solid state and film, respectively; Table 9). Ring-closing oxidation has been disclosed to be the main mechanism, reducing the fluorescence intensity, especially during summer.[124]

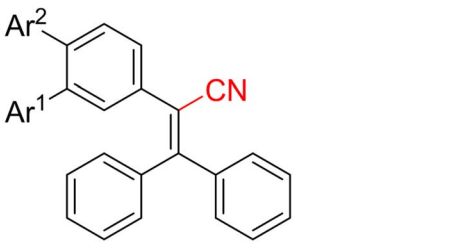

36a, Ar^1 = 2-methylphenyl, Ar^2 = H
36b, Ar^1 = phenyl, Ar^2 = H
36c, Ar^1 = 4-methoxyphenyl, Ar^2 = H
36d, Ar^1 = H, Ar^2 = 2-methylphenyl
36e, Ar^1 = H, Ar^2 = phenyl

Fig. 13 Triphenylacrylonitrile family of light conversion agents.

Tetraphenylethene (TPE) is another prominent scaffold used to construct organic light conversion agents. For instance, Qi *et al.* compared parent triphenylacrylonitrile with three TPE derivatives bearing carbazole peripheral donors, and it turned out that triphenylacrylonitrile outperformed all these derivatives in terms of excellent photostability and ultraviolet light conversion properties.[125]

Carbazole-functionalized cyanostilbene **37a–d** (Fig. 14) and structurally related phenanthrenecarbonitrile **37e** were investigated by Wang.[126] These luminophores showed various extents of AIE and *E*/*Z* isomerization of the central double bond. It was revealed that stilbenes **37a–d** are prone to Michael addition and intramolecular photocyclization reactions. In contrast, phenanthrenecarbonitrile **37e** does not undergo photocyclization, shows strong fluorescence in both the solid state and the film, and has high light-conversion efficiency (Table 9). Its high photostability is ascribed to a reduced electron density over the π-system due to the attached CN group, which decreases the electrophilicity of the whole

Table 9 Emissive properties of light conversion agents **36–38** for agricultural films

Light conversion agent	λ_{max}^{E} (nm)	Φ^F (%) (solid state)	Φ^F (%) (film)	Ref.
36a	*ca.* 385	57.60	5.40	124
36b	*ca.* 389	0.50	2.70	124
36c	*ca.* 375	0.40	2.90	124
36d	*ca.* 410	30.80	4.20	124
36e	*ca.* 400	83.30	10.70	124
Triphenylacrylonitrile	430	22.40	1.90	124/125
37a	454	—	15.00	126
37b	457	—	50.00	126
37c	455	—	18.00	126
37d	—	—	—	126
37e	449	—	65.00	126
TPE	478	25.32	—	125
38a	493	80.00	55.00	128
38b	485	83.00	52.00	128

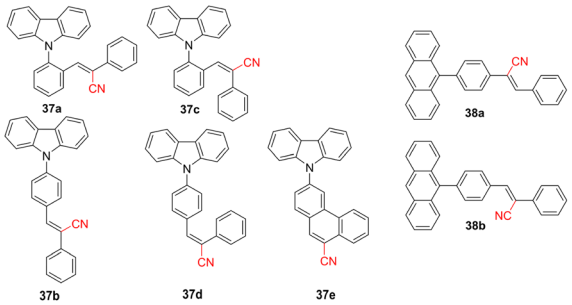

Fig. 14 Cyanostilbene and phenanthrenecarbonitrile light conversion agents.

system and its capability to accept electrons (an opposite effect of the carbazole moiety).[127] Anthracene-functionalized cyanostilbenes **38a**, **38b** were investigated for their polymorphism and potential application as light conversion agents for agricultural films. Especially isomer **38b** showed excellent matching of its fluorescence maxima (485 nm, Table 9), high fluorescence efficiency, and excellent photostability. The films doped with **38b** retained 94% of their initial intensity upon UV irradiation for 20 h.[128]

Supramolecular arrangement is another aspect to be considered when designing a light conversion agent. For instance, Yang *et al.* studied simple phenothiazine *N*-substituted benzonitrile, whose molecular packing significantly affected its room temperature phosphorescence (RTP). This simple luminogen crystallizes in three different crystalline polymorphs possessing different RTP lifetimes and photoluminescence quantum yields.[129] The molecular packing and AIE theory should be considered more broadly in the design of organic CN-functionalized molecules, as these may significantly affect general optoelectronic performance.[130,131]

Organic sensors and probes

Accurate, quick, and easy detection of various potentially hazardous analytes is of utmost importance to analytical and materials chemistry and imaging/biomedical techniques. In general, the detection should be sensitive with a low limit of detection (LOD), specific, non-invasive, low-cost, and should use non-ionizing irradiation. In this respect, colorimetric and fluorometric methods are well-established and widely used even for real-time monitoring. Fluorescence sensing technology has developed rapidly both *in vivo* and *in vitro*, and various fluorescent probes were recently developed, with many of them being biocompatible. Organic fluorescent probes are being routinely used as a general means to monitor molecular interactions across biochemistry, medicine, environmental science and industry.[132] These probes are usually composed of a prominent π-conjugated backbone/chromophore such as coumarin, xanthene (*e.g.*, fluorescein, eosin Y or rhodamine), porphyrin, phthalocyanine, cyanine, naphthalimide, fluoropyrrole, *etc.* along with a recognition acceptor and a spacer.[133–135] Cyano group connected to a π-conjugated system transmits its negative inductive and mesomeric effects that significantly influence absorption and emission properties. Hence, CN-capped colorimetric and fluorometric probes constitute another interesting class of organic molecules covered in this review. In principle, both electrophilic and nucleophilic species can be detected by CN-capped probes. For instance, Mu *et al.* developed a dual-response fluorescent probe **39** (Scheme 2) based on a rhodamine B scaffold functionalized by DCV recognition moiety. This probe can selectively detect hydrazine and cyanide, both environmentally and biologically relevant analytes. Whereas hydrazine detection is based on a replacement of malononitrile and the formation of hydrazone, cyanide adds to the DCV moiety. Both chemistries are accompanied by specific and easy-to-recognize changes in the emissive properties of the originally red-fluorescent probe **39**. Yellow or blue fluorescent products are formed upon the reaction with hydrazine or cyanide.[136]

Chemically identical detection mechanism of cyanide anions has also been utilized in D–π–A probe **40** (Scheme 3), utilizing both colorimetric and turn-on fluorescent sensing. The originally violet (amaranth) probe changes to yellow, allowing naked-eye detection of cyanide ions with the LOD of 1.4×10^{-8} M (Table 10). Moreover, the nucleophilic attack on the DCV moiety interrupts efficient ICT from the *N*,*N*-dimethylamino donor and turns on fluorescence appearing at 551 nm. A high selectivity and sensitivity towards cyanide ions over a wide range of competitive anions have been demonstrated. DCV-derivative **40** possesses low toxicity and has also been successfully applied in the bioimaging of living cells.[137]

Dicyanomethylene-4*H*-pyran (DCMP) is another widely employed moiety in organic fluorescent probes due to its peculiar optical properties, often reaching NIR region, large Stokes shifts, and photostability.[138] DCMP functionalized with thiophen-2-yl styrylcarboxylate **41** (Scheme 4) has been used to selectively detect cyanide ions even in the presence of interfering ions and small molecules. Whereas the original yellow probe **41** is not emissive, hydroxy derivative formed upon a hydrolytic cleavage of the ester function mediated by cyanide ions is green and possesses emission in the NIR region. Sensor **41** was found to be

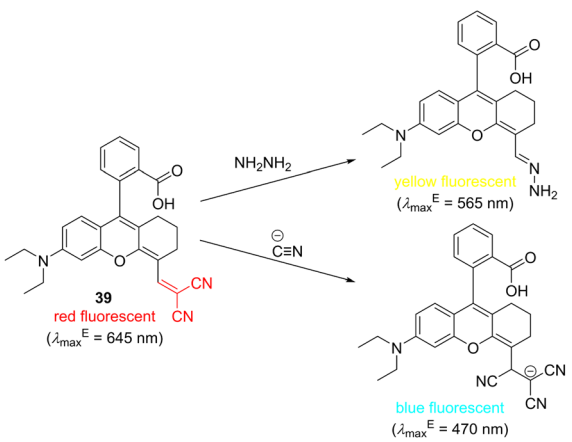

Scheme 2 Dual-response probe **39** based on rhodamine B equipped with DCV moiety.

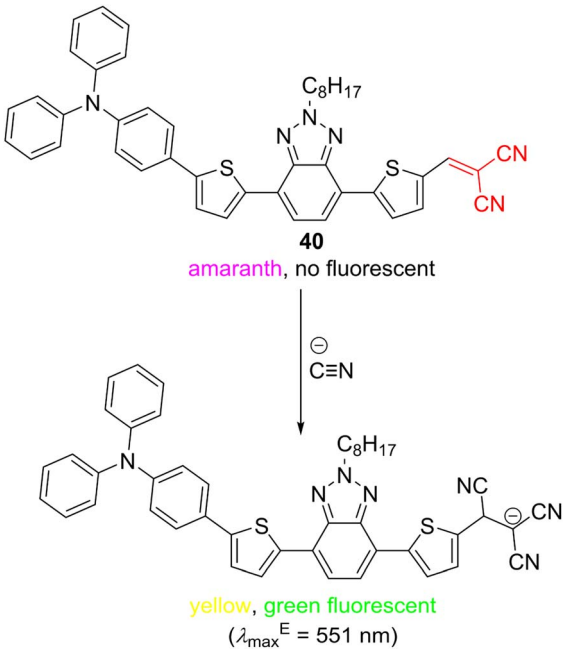

Scheme 3 Colorimetric and fluorometric detection of cyanide ions using probe **40**.

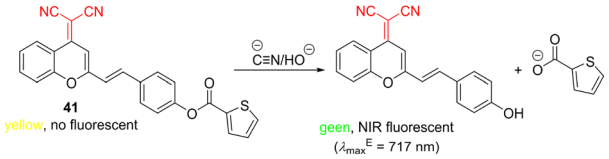

Scheme 4 DCMP-derived sensor of cyanide ions utilizing cleavage of ester function.

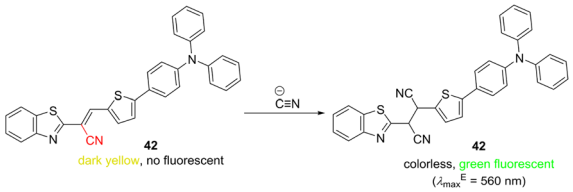

Scheme 5 Single cyano-capped probe **42** for detection of cyanide ions.

efficient in detecting cyanide in the intracellular region of MCF-7 cells[139] with the LOD of 1.44×10^{-6} M (Table 10).

Sensing methodologies of cyanide ions based on their nucleophilic addition reactions are significantly facilitated by the CN-functionalization of the probe structure.[140–142] Besides popular DCV-derived sensors, cyanovinyl analogue such as **42** are also feasible (Scheme 5). This push–pull molecule undergoes a nucleophilic addition solely with cyanide ions (LOD = 4.24×10^{-8} M, Table 10), leading to an interrupted ICT (decolorization) and pronounced emission at 560 nm. Furthermore, the detection of cyanide ions in living cells was possible due to low cytotoxicity of **42**.[143]

Besides nucleophiles, various electrophiles, mostly metal cations, can also be sensed by CN-capped organic probes. AIE-active molecules are increasingly popular in this respect.[144,145] For instance, simple DCV derivative **43**, prepared by Knoevenagel condensation of malononitrile and *N*,*N*-diethylaminobenzaldehyde, can be used for the detection of either cyanide anions or Fe^{3+} cations (Scheme 6). The original aggregated orange and fluorescent **43** was selectively decolorized by both analytes, accompanied by quenching/changing of the original emissive properties. The latter is due to the destruction of the original emissive aggregates either by producing a less rigid structure upon attaching the third CN group or by coordinating Fe^{3+} ions *via* DCV moiety and thus altering its electronic properties. It should be noted that the probe did not respond to Fe^{2+} ions.[146]

We have screened push–pull compound **44** for sensing various metal cations (Scheme 7), and it turned out that only Hg^{2+} and Cu^{2+} ions induce spectral changes. The original yellow color of **44** is decolorized/red-shifted in the presence of Hg^{2+}/Cu^{2+}. Whereas fluorescence properties persisted upon treatment with Hg^{2+}, no emission was observed for **44** and Cu^{2+}. Investigation of the sensing mechanism revealed N–S coordination of Hg^{2+} to imidazole/thiophene donor part, whereas Cu^{2+} in aqueous media induced hydrolysis of one of the CN groups present at the DCI moiety and subsequent formation of an imino derivative (IPIMO). In contrast to Cu^{2+}, Cu^{+} was inefficient in inducing such transformation. Hence, interrupting/enhancing efficient ICT in **44** resulted in either hypsochromic or bathochromic shifts of the absorption spectra accompanied by persisted or diminished emission. The LODs towards both ions are 0.16 and 0.03×10^{-6} M (Table 10). Moreover, paper strips coated with **44** were developed for a fast track detection of

Table 10 Overview of sensed species and LODs of organic fluorescent probes **39–44**

Probe	Sensed species 1	LOD (μM)	Sensing species 2	LOD (μM)	Ref.
39	N_2H_4	0.08	CN^-	0.33	136
40	CN^-	0.014	—	—	137
41	CN^-	1.44	—	—	139
42	CN^-	0.0424	—	—	143
43	Fe^{3+}	0.17	CN^-	0.39	146
44	Cu^{2+}	0.03	Hg^{2+}	0.16	147
45	DCP	0.20	DCNP	0.26	148

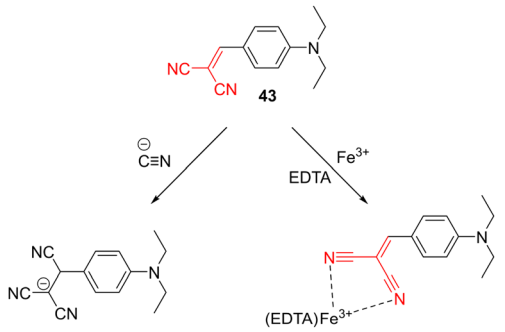

Scheme 6 Dual responsive probe **43** utilizing quenching/reduction of AIE as a detection mechanism.

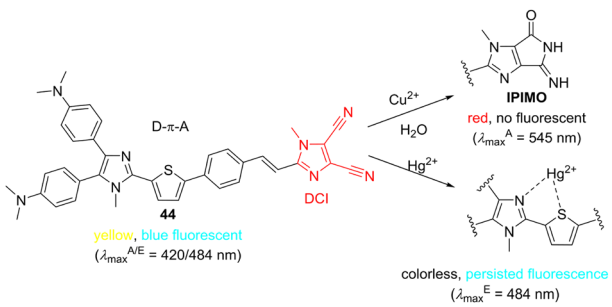

Scheme 7 Dicyanoimidazole D–π–A system capable of selectively detecting Cu^{2+} and Hg^{2+} ions.

both ions in real samples with the visualization either by naked-eye or handheld UV-lamp.[147]

Sensing of nerve gases is another important task to be addressed by organic probes. Y-shaped CN-capped NH-imidazole push–pull derivative **45** (Scheme 8) was revealed to detect sarin and tabun mimics DCP and DCNP very selectively. The originally weakly emissive aggregates of **45** react quickly with DCP/DCNP in terms of nucleophilic substitution, affording highly emissive *N*-phosphorylated adduct, which underwent slow hydrolysis in aqueous media to **45H**$^+$ and nontoxic phosphoric acid derivative. Hence, **45** is able to detect and detoxify both mimics of nerve gases with the LODs of 0.20 and 0.26 × 10^{-6} M (Table 10), respectively.[148]

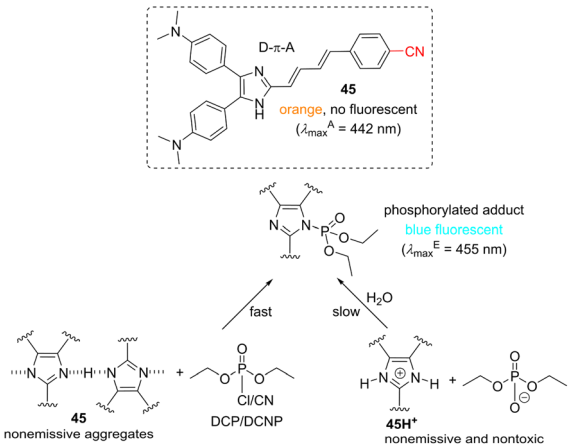

Scheme 8 Molecular structure of sensor **45** and its mechanism of detection and detoxification of nerve gases.

Photoredox catalysis

The use of visible light in organic synthesis is considered a green and sustainable source of energy, allowing radical processes that recently came back to the foreground as photoredox catalysis. Its renaissance has been due to synthetically attractive visible light-initiated radical transformations that can be accomplished at very mild reaction conditions. The current photoredox catalysis relies on a suitable catalyst, which undergoes facile excitation by visible light to yield a strong one-electron reducing or oxidizing reagent. Ru- and Ir-polypyridyl complexes are traditional and efficient photoredox catalysts but their use can be, in particular cases, limited by the presence of heavy metals and their high costs.[149–151] In this respect, organic photoredox catalysis seems to be a greener way of utilizing purely organic catalysts such as xanthene dyes (*e.g.*, Eosin Y, Fluorescein, Rose Bengal), flavins, perylenediimide, acridiniums, and last but not the least dicyano(hetero)arenes. The latter cyano-capped synthetic dyes attract particular attention due to their easily tunable properties.[152–154] Fig. 15 shows the molecular structure of typical CN-substituted aromatic (hetero)cycles, including two major groups – dicyanobenzene/naphthalene/anthracene **46–50** and dicyanopyrazines **51**. Their fundamental photophysical properties are summarized in Table 11. The absorption maxima are important parameters used to fit the catalyst with a suitable light source, whereas the ground- and excited-state electrochemical properties are crucial to determine the fundamental redox potentials and subsequently estimate the feasibility of a desired photoredox process.

Photophysics of cyanoarenes is well investigated, and compounds **46–48** represent photoredox catalysts enabling electron transfer from the singlet excited state. Due to their high ground state reduction potentials ranging from −1.46 to −0.91 V (Table 11), these simple dinitriles also possess high

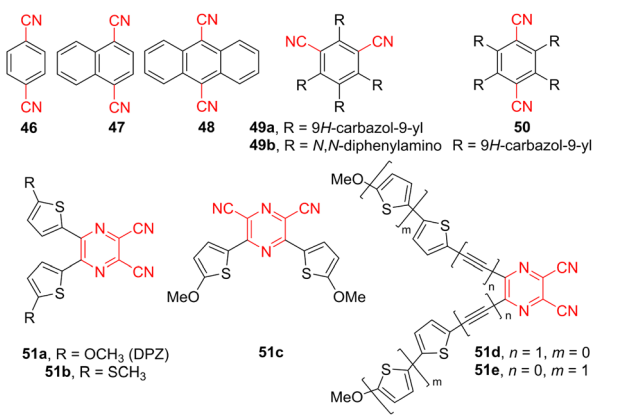

Fig. 15 The molecular structure of CN-capped photoredox catalysts – cyanoarenes **46–50** and DPZs **51**.

Table 11 Fundamental photophysical properties of photoredox catalysts **46–51**

Catalysts	λ_{max}^{A} (nm eV^{-1})	$E_{0,0}$ (eV)	Ground state redox potentials (*V vs.* SCE)		Excited state redox potentials[a] (*V vs.* SCE)		Ref.
			$E_{1/2(red)}$	$E_{1/2(ox)}$	E^{*}_{red}	E^{*}_{ox}	
46	290/4.28	4.01	−1.46	—	+2.55	—	153
47	325/3.82	3.57	−1.27	—	+2.30	—	153
48	422/2.94	2.90	−0.91	—	+1.99	—	153
49a	435/2.85	2.56	−1.04	+1.35	+1.52	−1.21	153
49b	425/2.92	2.62	−1.28	+1.10	+1.34	−1.52	153
50	463/2.68	2.43	−0.99	+1.41	+1.44	−1.02	153
51a	440/2.82	2.50	−1.14	+1.32	+1.36	−1.18	160
51b	443/2.79	2.22	−1.01	+1.32	+1.21	−0.90	160
51c	389/3.19	2.70	−1.15	+1.57	+1.55	−1.13	160
51d	459/2.70	2.59	−0.80	+1.46	+1.82	−1.16	161
51e	511/2.43	—	−0.95	+1.11	—	—	161

[a] Singlet excited state redox potentials.

singlet excited energies $E_{0,0}$. Extended cyanoarenes (*e.g.*, **46** *vs.* **48**) are better suited to photoredox catalysis due to their red-shifted absorption maxima and longer lifetimes of the singlet excited state. Amino-substituted dicyanobenzenes **49** and **50** bearing either 9*H*-carbazol-9-yl or *N*,*N*-diphenylamino donors are relatively new D–π–A photoredox catalysts.[155] Especially catalyst **49a** (4CzIPN) has been thoroughly explored in a plethora of photoredox transformations.[156] Its further structural tuning by replacing the donor or isomerization afforded derivatives **49b** and **50**.[157] A replacement of carbazole by *N*,*N*-diphenylamino group (**49a** → **49b**) led to lowered redox potentials (−1.28 and +1.10 V, Table 11), whereas isomerization of **49a** to **50** slightly increased the redox potentials and red-shifted the absorption maxima to 463 nm. 5,6-Disubstituted pyrazine-2,3-dicarbonitriles **51a–e** (DPZ, Fig. 15) represent the family of heteroaromatic photoredox catalysts with two cyano acceptors and two methoxy/methylthiothiophene donors recently developed in our group.[158] These catalysts evolved from dicyanopyrazine NLOphores **30** (Fig. 10) by further structural tuning. Especially the parent DPZ catalyst **51a** showed very broad application potential across various photochemical transformations, including C–C bond formation,[159–163] enantioselective photoreduction,[164,165] pH controlled photooxygenation of indoles,[166] *etc.* Its structure has been further systematically modified by varying the peripheral donor (OMe → SMe, **51a** → **51b**), which affected the reduction/oxidation potentials of the excited state, and subsequently, also the excited state energy. Isomerization of substituents along the pyrazine core (**51a** → **51c**) significantly influenced the chromophore arrangement resulting in the merging of two original absorption bands (λ_{max}^{A} = 440 and 360 nm) seen for **51a** into a single band of **51c** appearing at 389 nm. Further extension and planarization of the π-system by additional acetylenic spacers, as in **51d** resulted in slightly red-shifted absorption and increased $E_{0,0}$. The attachment of methoxy-substituted bithiophene linker (**51e**) significantly supported the ICT, suppressed emissive properties, and red-shifted the absorption maxima to 511 nm. Hence, structural variation of CN-capped aromatic (hetero)cycles **46–51** allowed extensive tuning of their photoredox properties.

Conclusions

Due to its negative inductive and mesomeric effects, the cyano group can significantly alter the electronic properties of π-conjugated systems and CN can be denoted as a linear and increasingly popular electron acceptor. Six fundamental groups of CN-capped small organic materials were reviewed, including materials applicable in OSCs, OLEDs, NLO, light conversion agents, organic sensors and probes, and photoredox catalysis. Semiconductors used as acceptors in solar cells may contain either single-CN group(s) or DCV moiety. The latter is often part of larger scaffolds such as (F)IC or dicyanorhodanine with pronounced electron-withdrawing properties. The cyano-capped semiconductors usually possess reduced LUMO level, narrowed bandgap, and red-shifted absorption and thus enhanced device efficiency with the PCE reaching up to 12%. Organic emitters for OLEDs can be easily tuned by attaching CN groups, either single DCV moiety, and achieve a device with improved luminance, well-tailored color, and EQE up to 12%. Cyano-substituted push–pull molecules possess long-lasting tradition in nonlinear optics; a variety of novel and complex CN-based acceptors were recently developed, including cyanoaryls, dicyanoimidazole, (di)cyanothiophene, dicyanopyrazine/benzene, tricyanofuran, *etc.* These moieties allow the construction of D–π–A systems with the ICT of a large extent and thus of different NLO responses. Nowadays, organic light conversion agents are a burgeoning area of π-conjugated compounds used to produce agricultural films affecting plant growth. Triphenylacrylonitrile and related cyanostilbenes are the most popular CN-capped molecules capable of converting unproductive ultraviolet and yellow-green wavelengths into red-orange and blue-violet light. Organic sensors and probes are being used to detect various analytes. For instance, DCV-substituted molecules undergo facile addition of cyanide ions resulting in a product with different optical properties. Hence,

colorimetric and fluorometric detection of this environmentally important analyte is possible. DCI-based push–pull molecules proved to be very selective detectors of Cu^{2+} ions, and CN-capped imidazoles also detect and detoxify nerve gases. The group of cyano-substituted compounds is cyanoarenes and X-shaped dicyanopyrazines, which were recently applied as very efficient and pure organic photoredox catalysts. These synthetic dyes possess tunable structures and properties, and their visible light-induced catalytic activity has been demonstrated in various organic transformations.

The aforementioned examples clearly revealed organic CN-capped compounds as versatile organic materials, and attaching the cyano group represents well-established structural tuning used across various branches of the current materials chemistry.

Author contributions

H. W., C. Z. and J. L.: conceptualization. H. W., C. Z. and Z. B.: data curation. H. W., F. B. and J. L.: formal analysis. F. B. and J. L.: funding acquisition. H. W., C. Z., Z. B. and F. B.: investigation. F. B. and J. L.: project administration. J. L.: supervision. H. W. and F. B.: writing-original draft. H. W., C. Z., Z. B., F. B. and J. L.: writing-review & editing.

Conflicts of interest

There are no conflicts to declare.

Note added after first publication

This article replaces the version published on 31st January 2023, which contained an incorrect version of Fig. 10.

Acknowledgements

This work was supported by the Science and technology project of Inner Mongolia Autonomous Region (2021GG0063), Finance Science and Technology Project of Hainan Province (No. ZDYF2020084), Central Public-interest Scientific Institution Basal Research Fund (No. BSRF202105), Key scientific and technological projects of Xinjiang Production and Construction Corps (No. 2021AB007), Science and Technology Project of the Ninth Agricultural Division of Xinjiang Production and Construction Corps (2020JS015), and Changzhou Science and Technology Program (No. CE20202022). ZB and FB are indebted to the Czech Science Foundation (22-14988S).

Notes and references

1 F. Bureš, *Chem. Listy*, 2013, **107**, 834–842.
2 F. Bureš, *RSC Adv.*, 2014, **4**, 58826–58851.
3 Y. Wu and W. Zhu, *Chem. Soc. Rev.*, 2013, **42**, 2039–2058.
4 H. Cha, H. N. Kim, T. K. An, M. S. Kang, S.-K. Kwon, Y.-H. Kim and C. E. Park, *ACS Appl. Mater. Interfaces*, 2014, **6**, 15774–15782.
5 H. Li, M. Fang, Y. Hou, R. Tang, Y. Yang, C. Zhong, Q. Li and Z. Li, *ACS Appl. Mater. Interfaces*, 2016, **8**, 12134–12140.
6 X. Tang, X.-L. Li, H. Liu, Y. Gao, Y. Shen, S. Zhang, P. Lu, B. Yang, S.-J. Su and Y. Ma, *Dyes Pigm.*, 2018, **149**, 430–436.
7 Y. Rahmawati, A. Afandi, D. Arengga, S. Sendari, W. Agustin, T. Matsumoto and I. Rahman, *IOP Conf. Ser. Earth Environ. Sci.*, 2018, **105**, 012079.
8 D. M. Kammen, *Sci. Am.*, 2006, **295**, 84–93.
9 V. Balzani, A. Credi and M. Venturi, *ChemSusChem*, 2008, **1**, 26–58.
10 C. J. Brabec, N. S. Sariciftci and J. C. Hummelen, *Adv. Funct. Mater.*, 2001, **11**, 15–26.
11 S. Günes, H. Neugebauer and N. S. Sariciftci, *Chem. Rev.*, 2007, **107**, 1324–1338.
12 Y.-J. Cheng, S.-H. Yang and C.-S. Hsu, *Chem. Rev.*, 2009, **109**, 5868–5923.
13 A. W. Hains, Z. Liang, M. A. Woodhouse and B. A. Gregg, *Chem. Rev.*, 2010, **110**, 6689–6735.
14 S. Dey, *Small*, 2019, **15**, 1900134.
15 C. W. Tang, *Appl. Phys. Lett.*, 1986, **48**, 183–185.
16 A. Shah, P. Torres, R. Tscharner, N. Wyrsch and H. Keppner, *Science*, 1999, **285**, 692–698.
17 G. Dennler, M. C. Scharber and C. J. Brabec, *Adv. Mater.*, 2009, **21**, 1323–1338.
18 D. Gendron and M. Leclerc, *Energy Environ. Sci.*, 2011, **4**, 1225–1237.
19 C. Duan, F. Huang and Y. Cao, *J. Mater. Chem.*, 2012, **22**, 10416–10434.
20 J. You, L. Dou, K. Yoshimura, T. Kato, K. Ohya, T. Moriarty, K. Emery, C.-C. Chen, J. Gao and G. Li, *Nat. Commun.*, 2013, **4**, 1–10.
21 Y. Liang, Z. Xu, J. Xia, S. T. Tsai, Y. Wu, G. Li, C. Ray and L. Yu, *Adv. Mater.*, 2010, **22**, E135–E138.
22 T. Taima, M. Chikamatsu, Y. Yoshida, K. Saito and K. Yase, *Appl. Phys. Lett.*, 2004, **85**, 1832–1834.
23 Y. Zhang, B. Kan, Y. Sun, Y. Wang, R. Xia, X. Ke, Y. Q. Q. Yi, C. Li, H. L. Yip and X. Wan, *Adv. Mater.*, 2018, **30**, 1707508.
24 F. Zhao, S. Dai, Y. Wu, Q. Zhang, J. Wang, L. Jiang, Q. Ling, Z. Wei, W. Ma and W. You, *Adv. Mater.*, 2017, **29**, 1700144.
25 L. Meng, Y. Zhang, X. Wan, C. Li, X. Zhang, Y. Wang, X. Ke, Z. Xiao, L. Ding and R. Xia, *Science*, 2018, **361**, 1094–1098.
26 W. Zhao, S. Li, H. Yao, S. Zhang, Y. Zhang, B. Yang and J. Hou, *J. Am. Chem. Soc.*, 2017, **139**, 7148–7151.
27 S. Zhang, Y. Qin, J. Zhu and J. Hou, *Adv. Mater.*, 2018, **30**, 1800868.
28 K. Jiang, J. Zhang, C. Zhong, F. R. Lin, F. Qi, Q. Li, Z. Peng, W. Kaminsky, S.-H. Jang and J. Yu, *Nat. Energy*, 2022, **7**, 1076–1086.
29 Y. Ie, S. Jinnai, M. Karakawa and Y. Aso, *Chem. Lett.*, 2015, **44**, 694–696.
30 Y. Shibata, T. Kono, H. Usui and Y. Yoshida, *Chem. Lett.*, 2015, **44**, 680–682.
31 W. Jiang, L. Ye, X. Li, C. Xiao, F. Tan, W. Zhao, J. Hou and Z. Wang, *Chem. Commun.*, 2014, **50**, 1024–1026.
32 G. Sharma, M. Roy, J. Mikroyannidis and K. J. Thomas, *Org. Electron.*, 2012, **13**, 3118–3129.

33 Y. Zhou, L. Ding, K. Shi, Y. Z. Dai, N. Ai, J. Wang and J. Pei, *Adv. Mater.*, 2012, **24**, 957–961.
34 Y.-Q. Zheng, Y.-Z. Dai, Y. Zhou, J.-Y. Wang and J. Pei, *Chem. Commun.*, 2014, **50**, 1591–1594.
35 S. Li, J. Yan, C.-Z. Li, F. Liu, M. Shi, H. Chen and T. P. Russell, *J. Mater. Chem. A*, 2016, **4**, 3777–3783.
36 M. Klikar, V. Jelínková, Z. Růžičková, T. Mikysek, O. Pytela, M. Ludwig and F. Bureš, *Eur. J. Org. Chem.*, 2017, **2017**, 2764–2779.
37 S. P. Singh, *J. Mater. Chem. A*, 2019, **7**, 22701–22729.
38 K. Wang, Y. Firdaus, M. Babics, F. Cruciani, Q. Saleem, A. El Labban, M. A. Alamoudi, T. Marszalek, W. Pisula and F. Laquai, *Chem. Mater.*, 2016, **28**, 2200–2208.
39 T. Duan, M. Babics, A. Seitkhan, Y. Firdaus, R.-Z. Liang, F. Cruciani, S. Liu, S. Lopatin and P. M. Beaujuge, *J. Mater. Chem. A*, 2018, **6**, 9368–9372.
40 W. Zhao, S. Li, H. Yao, S. Zhang, Y. Zhang, B. Yang and J. Hou, *J. Am. Chem. Soc.*, 2017, **139**, 7148–7151.
41 S. j. Xu, Z. Zhou, W. Liu, Z. Zhang, F. Liu, H. Yan and X. Zhu, *Adv. Mater.*, 2017, **29**, 1704510.
42 J. Sun, X. Ma, Z. Zhang, J. Yu, J. Zhou, X. Yin, L. Yang, R. Geng, R. Zhu and F. Zhang, *Adv. Mater.*, 2018, **30**, 1707150.
43 B. Al-Anesi, S. Revoju, A. Hiltunen, R. Suhonen, T. M. Kraft, M. Liu, H. Zhang, Z. Deng, C. Fedele and A. Berdin, *Energy Technol.*, 2022, **10**, 2200264.
44 Y. Zhou, M. Li, H. Lu, H. Jin, X. Wang, Y. Zhang, S. Shen, Z. Ma, J. Song and Z. Bo, *Adv. Funct. Mater.*, 2021, **31**, 2101742.
45 H. Hang, X. Wu, Q. Xu, Y. Chen, H. Li, W. Wang, H. Tong and L. Wang, *Dyes Pigm.*, 2019, **160**, 243–251.
46 Y. Li, L. Zhong, F.-P. Wu, Y. Yuan, H.-J. Bin, Z.-Q. Jiang, Z. Zhang, Z.-G. Zhang, Y. Li and L.-S. Liao, *Energy Environ. Sci.*, 2016, **9**, 3429–3435.
47 Y. Lin, J. Wang, Z. G. Zhang, H. Bai, Y. Li, D. Zhu and X. Zhan, *Adv. Mater.*, 2015, **27**, 1170–1174.
48 S. Li, L. Ye, W. Zhao, S. Zhang, S. Mukherjee, H. Ade and J. Hou, *Adv. Mater.*, 2016, **28**, 9423–9429.
49 Y. Li, X. Liu, F.-P. Wu, Y. Zhou, Z.-Q. Jiang, B. Song, Y. Xia, Z.-G. Zhang, F. Gao and O. Inganäs, *J. Mater. Chem. A*, 2016, **4**, 5890–5897.
50 C. e. Zhang, S. Feng, Y. Liu, R. Hou, Z. Zhang, X. Xu, Y. Wu and Z. Bo, *ACS Appl. Mater. Interfaces*, 2017, **9**, 33906–33912.
51 Z. Zhang, W. Liu, T. Rehman, H.-X. Ju, J. Mai, X. Lu, M. Shi, J. Zhu, C.-Z. Li and H. Chen, *J. Mater. Chem. A*, 2017, **5**, 9649–9654.
52 Y. Yang, Z.-G. Zhang, H. Bin, S. Chen, L. Gao, L. Xue, C. Yang and Y. Li, *J. Am. Chem. Soc.*, 2016, **138**, 15011–15018.
53 W. T. Hadmojo, F. T. A. Wibowo, D. Y. Ryu, I. H. Jung and S.-Y. Jang, *ACS Appl. Mater. Interfaces*, 2017, **9**, 32939–32945.
54 B. Xiao, J. Song, B. Guo, M. Zhang, W. Li, R. Zhou, J. Liu, H.-B. Wang, M. Zhang and G. Luo, *J. Mater. Chem. A*, 2018, **6**, 957–962.
55 X. Xu, T. Yu, Z. Bi, W. Ma, Y. Li and Q. Peng, *Adv. Mater.*, 2018, **30**, 1703973.
56 Y. Lin, F. Zhao, Y. Wu, K. Chen, Y. Xia, G. Li, S. K. Prasad, J. Zhu, L. Huo, H. Bin, Z. G. Zhang, X. Guo, M. Zhang, Y. Sun, F. Gao, Z. Wei, W. Ma, C. Wang, J. Hodgkiss, Z. Bo, O. Inganäs, Y. Li and X. Zhan, *Adv. Mater.*, 2017, **29**, 1604155.
57 B. Guo, W. Li, X. Guo, X. Meng, W. Ma, M. Zhang and Y. Li, *Adv. Mater.*, 2017, **29**, 1702291.
58 H. Bin, Y. Yang, Z.-G. Zhang, L. Ye, M. Ghasemi, S. Chen, Y. Zhang, C. Zhang, C. Sun and L. Xue, *J. Am. Chem. Soc.*, 2017, **139**, 5085–5094.
59 Y.-C. Lin, N.-Z. She, C.-H. Chen, A. Yabushita, H. Lin, M.-H. Li, B. Chang, T.-F. Hsueh, B.-S. Tsai and P.-T. Chen, *ACS Appl. Mater. Interfaces*, 2022, **14**, 37990–38003.
60 J. Huang, H. Tang, C. Yan and G. Li, *Cell Rep. Phys. Sci.*, 2021, **2**, 100292.
61 Y. Cui, Y. Wang, J. Bergqvist, H. Yao, Y. Xu, B. Gao, C. Yang, S. Zhang, O. Inganäs and F. Gao, *Nat. Energy*, 2019, **4**, 768–775.
62 V. Gupta, A. Bagui and S. P. Singh, *Adv. Funct. Mater.*, 2017, **27**, 1603820.
63 A. Bagui, A. Garg, B. Tyagi, V. Gupta and S. P. Singh, *Chem. Commun.*, 2018, **54**, 4001–4004.
64 H. Xu, Y. Yang, C. Zhong, X. Zhan and X. Chen, *J. Mater. Chem. A*, 2018, **6**, 6393–6401.
65 I. D. W. Samuel and G. A. Turnbull, *Chem. Rev.*, 2007, **107**, 1272–1295.
66 Y. Shao, G. C. Bazan and A. J. Heeger, *Adv. Mater.*, 2008, **20**, 1191–1193.
67 C. R. Newman, C. D. Frisbie, D. A. da Silva Filho, J.-L. Brédas, P. C. Ewbank and K. R. Mann, *Chem. Mater.*, 2004, **16**, 4436–4451.
68 Z. Chi, X. Zhang, B. Xu, X. Zhou, C. Ma, Y. Zhang, S. Liu and J. Xu, *Chem. Soc. Rev.*, 2012, **41**, 3878–3896.
69 L. Yan, Y. Zhang, B. Xu and W. Tian, *Nanoscale*, 2016, **8**, 2471–2487.
70 X. Li, K. Ma, S. Zhu, S. Yao, Z. Liu, B. Xu, B. Yang and W. Tian, *Anal. Chem.*, 2014, **86**, 298–303.
71 C. W. Tang and S. A. VanSlyke, *Appl. Phys. Lett.*, 1987, **51**, 913–915.
72 M. Y. Wong and E. Zysman-Colman, *Adv. Mater.*, 2017, **29**, 1605444.
73 X. Cao, D. Zhang, S. Zhang, Y. Tao and W. Huang, *J. Mater. Chem. C*, 2017, **5**, 7699–7714.
74 D. U. Kim, S. H. Paik, S.-H. Kim and T. Tsutsui, *Synth. Met.*, 2001, **123**, 43–46.
75 L. Hung and C. Chen, *Mater. Sci. Eng., R*, 2002, **39**, 143–222.
76 S. Zhang, L. Yao, Q. Peng, W. Li, Y. Pan, R. Xiao, Y. Gao, C. Gu, Z. Wang and P. Lu, *Adv. Funct. Mater.*, 2015, **25**, 1755–1762.
77 J. Y. Hu, Y. J. Pu, F. Satoh, S. Kawata, H. Katagiri, H. Sasabe and J. Kido, *Adv. Funct. Mater.*, 2014, **24**, 2064–2071.
78 S. J. Cha, N. S. Han, J. K. Song, S.-R. Park, Y. M. Jeon and M. C. Suh, *Dyes Pigm.*, 2015, **120**, 200–207.
79 X. Tao, S. Miyata, H. Sasabe, G. Zhang, T. Wada and M. Jiang, *Appl. Phys. Lett.*, 2001, **78**, 279–281.
80 T.-H. Liu, C.-Y. Iou and C. H. Chen, *Appl. Phys. Lett.*, 2003, **83**, 5241–5243.

81 P. Franken, A. E. Hill, C. e. Peters and G. Weinreich, *Phys. Rev. Lett.*, 1961, **7**, 118.
82 R. W. Hellwarth, *Phys. Rev.*, 1963, **130**, 1850.
83 R. Chiao, C. Townes and B. Stoicheff, *Phys. Rev. Lett.*, 1964, **12**, 592.
84 H. Durr and H. Bouas-Laurent, *Photochromism: Molecules and Systems*, Elsevier, 2003.
85 J. A. Delaire and K. Nakatani, *Chem. Rev.*, 2000, **100**, 1817–1846.
86 D. R. Kanis, M. A. Ratner and T. J. Marks, *Chem. Rev.*, 1994, **94**, 195–242.
87 M. Gimeno, A. Laguna and T. Meyer, *Comprehensive Coordination Chemistry II*, Elsevier, Oxford, 2004, vol. 6, p. 1.
88 J. Zyss, *Molecular Nonlinear Optics: Materials, Physics, and Devices*, Academic press, 2013.
89 C. Bosshard, K. Sutter, P. Prêtre, J. Hulliger, M. Flörsheimer, P. Kaatz and P. Günter, *Organic Nonlinear Optical Materials*, CRC press, 2020.
90 S. R. Marder, *Chem. Commun.*, 2006, 131–134.
91 M. G. Papadopoulos, A. J. Sadlej and J. Leszczynski, *Nonlinear Optical Properties of Matter*, Springer, 2006.
92 W. Gong, Q. Li, Z. Li, C. Lu, J. Zhu, S. Li, J. Yang, Y. Cui and J. Qin, *J. Phys. Chem. B*, 2006, **110**, 10241–10247.
93 J. L. Bredas, C. Adant, P. Tackx, A. Persoons and B. Pierce, *Chem. Rev.*, 1994, **94**, 243–278.
94 S. D. Bella, *Chem. Soc. Rev.*, 2001, **30**, 355–366.
95 V. Guieu, C. Payrastre, Y. Madaule, S. Garcia-Alonso, P. G. Lacroix and K. Nakatani, *Chem. Mater.*, 2006, **18**, 3674–3681.
96 L. R. Dalton, P. A. Sullivan and D. H. Bale, *Chem. Rev.*, 2010, **110**, 25–55.
97 P. A. Sullivan and L. R. Dalton, *Acc. Chem. Res.*, 2010, **43**, 10–18.
98 B. H. Robinson, L. E. Johnson, D. L. Elder, A. A. Kocherzhenko, C. M. Isborn, C. Haffner, W. Heni, C. Hoessbacher, Y. Fedoryshyn and Y. Salamin, *J. Lightwave Technol.*, 2018, **36**, 5036–5047.
99 J. Liu, C. Ouyang, F. Huo, W. He and A. Cao, *Dyes Pigm.*, 2020, **181**, 108509.
100 M. Klikar, P. Solanke, J. Tydlitát and F. Bureš, *Chem. Rec.*, 2016, **16**, 1886–1905.
101 J. Kulhánek and F. Bureš, *Beilstein J. Org. Chem.*, 2012, **8**, 25–49.
102 D. Cvejn, E. Michail, I. Polyzos, N. Almonasy, O. Pytela, M. Klikar, T. Mikysek, V. Giannetas, M. Fakis and F. Bureš, *J. Mater. Chem. C*, 2015, **3**, 7345–7355.
103 J. Kulhánek, F. Bureš, O. Pytela, T. Mikysek, J. Ludvík and A. Růžička, *Dyes Pigm.*, 2010, **85**, 57–65.
104 A. Plaquet, B. Champagne, J. Kulhánek, F. Bureš, E. Bogdan, F. Castet, L. Ducasse and V. Rodriguez, *ChemPhysChem*, 2011, **12**, 3245–3252.
105 J. Kulhánek, F. Bures, A. Wojciechowski, M. Makowska-Janusik, E. Gondek and I. Kityk, *J. Phys. Chem. A*, 2010, **114**, 9440–9446.
106 F. Bureš, J. Kulhánek, T. Mikysek, J. Ludvík and J. Lokaj, *Tetrahedron Lett.*, 2010, **51**, 2055–2058.
107 J. Kulhánek, F. Bureš, W. Kuznik, I. V. Kityk, T. Mikysek and A. Růžička, *Chem.–Asian J.*, 2013, **8**, 465–475.
108 L. Dokládalová, F. Bureš, W. Kuznik, I. V. Kityk, A. Wojciechowski, T. Mikysek, N. Almonasy, M. Ramaiyan, Z. Padělková and J. Kulhánek, *Org. Biomol. Chem.*, 2014, **12**, 5517–5527.
109 F. Bureš, H. Čermáková, J. Kulhánek, M. Ludwig, W. Kuznik, I. V. Kityk, T. Mikysek and A. Růžička, *Eur. J. Org. Chem.*, 2012, **2012**, 529–538.
110 W. Gong, Q. Li, S. Li, C. Lu, Z. Li, J. Zhu, Z. Zhu, Q. Wang, Y. Cui and J. Qin, *Mater. Lett.*, 2007, **61**, 1151–1153.
111 Y. Yang, H. Xiao, H. Wang, F. Liu, S. Bo, J. Liu, L. Qiu, Z. Zhen and X. Liu, *J. Mater. Chem. C*, 2015, **3**, 11423–11431.
112 J. Liu, M. Zhang, W. Gao, A. Fedorchuk and I. Kityk, *J. Mol. Struct.*, 2018, **1165**, 223–227.
113 Y. Yang, H. Xu, F. Liu, H. Wang, G. Deng, P. Si, H. Huang, S. Bo, J. Liu and L. Qiu, *J. Mater. Chem. C*, 2014, **2**, 5124–5132.
114 Z. a. Li, H. Kim, S.-H. Chi, J. M. Hales, S.-H. Jang, J. W. Perry and A. K.-Y. Jen, *Chem. Mater.*, 2016, **28**, 3115–3121.
115 W. Wang, X. Yang and S. Xiao, *J. Lumin.*, 2020, **225**, 117406.
116 H. Wang, S. Yang, X. Li, F. Yang, X. Sun, W. Li and Z. Yao, *Polym.-Plast. Technol. Mater.*, 2020, **59**, 1875–1886.
117 Y. Yu, P. Xu, S. Jia, H. Pan, H. Zhang, D. Wang and L. Dong, *Int. J. Biol. Macromol.*, 2019, **127**, 210–221.
118 H. I. Yoon, J. H. Kim, K. S. Park, J. W. Namgoong, T. G. Hwang, J. P. Kim and J. E. Son, *Hortic., Environ. Biotechnol.*, 2020, **61**, 999–1009.
119 Y. Jiang, C. Yan, H. Zhang, M. Wu, S. Zheng, Y. Zhang and L. Xu, *Coatings*, 2021, **11**, 139.
120 D. Wang, Y. Yu, X. Ai, H. Pan, H. Zhang and L. Dong, *Polym. Adv. Technol.*, 2019, **30**, 203–211.
121 T. G. Hwang, J. Y. Kim, J. W. Namgoong, J. M. Lee, S. B. Yuk, S. H. Kim and J. P. Kim, *Photochem. Photobiol. Sci.*, 2019, **18**, 1064–1074.
122 Y. Liu, J. Liu, Q. Liu, W. He and I. Kityk, *J. Lumin.*, 2020, **218**, 116852.
123 Y. Liu, Z. Gui and J. Liu, *Polymers*, 2022, **14**, 851.
124 Y. Wang, Y. Yu, W. Liu, L. Ren and G. Ge, *J. Agric. Food Chem.*, 2018, **66**, 13295–13302.
125 Y. Qi, Y. Wang, Y. Yu, Z. Liu, Y. Zhang, Y. Qi and C. Zhou, *J. Mater. Chem. C*, 2016, **4**, 11291–11297.
126 Y. Wang, Z. Qian, X. Li, A. Qin, Y. Guo and B. Tang, *J. Mater. Chem. C*, 2021, **9**, 12681–12693.
127 M. L. Kadam, D. Patil and N. Sekar, *Opt. Mater.*, 2018, **85**, 308–318.
128 Y. Wang, Z. Qian, X. Li, A. Qin, Y. Guo and B. Tang, *Dyes Pigm.*, 2022, **197**, 109888.
129 J. Yang, Z. Ren, B. Chen, M. Fang, Z. Zhao, B. Z. Tang, Q. Peng and Z. Li, *J. Mater. Chem. C*, 2017, **5**, 9242–9246.
130 Q. Li and Z. Li, *Acc. Chem. Res.*, 2020, **53**, 962–973.
131 J. Mei, N. L. Leung, R. T. Kwok, J. W. Lam and B. Z. Tang, *Chem. Rev.*, 2015, **115**, 11718–11940.
132 H. Zhang, D. C. Salo, D. M. Kim, S. Komarov, Y.-C. Tai and M. Y. Berezin, *J. Biomed. Opt.*, 2016, **21**, 126006.
133 L. Yuan, W. Lin, K. Zheng, L. He and W. Huang, *Chem. Soc. Rev.*, 2013, **42**, 622–661.

134 H. Kobayashi, Y. Koyama, T. Barrett, Y. Hama and P. L. Choyke, Molecular Probes for Biomedical Applications II, *Proc. SPIE*, 2008, **6867**, 157–164.
135 J. Chan, S. C. Dodani and C. J. Chang, *Nat. Chem.*, 2012, **4**, 973–984.
136 S. Mu, H. Gao, C. Li, S. Li, Y. Wang, Y. Zhang, C. Ma, H. Zhang and X. Liu, *Talanta*, 2021, **221**, 121606.
137 Q. Li, Z. Wang, W. Song, H. Ma, J. Dong, Y.-Y. Quan, X. Ye and Z.-S. Huang, *Dyes Pigm.*, 2019, **161**, 389–395.
138 X. Yang, Y. Liu, Y. Wu, X. Ren, D. Zhang and Y. Ye, *Sens. Actuators, B*, 2017, **253**, 488–494.
139 B.-B. Wang, Y. Wang, W.-N. Wu, Z.-H. Xu, X.-L. Zhao, Z.-Q. Xu and Y.-C. Fan, *Inorg. Chem. Commun.*, 2020, **122**, 108245.
140 Q. Wu, S. Wang, E. Hao and L. Jiao, *Spectrochim. Acta, Part A*, 2021, **247**, 119102.
141 A. Tigreros and J. Portilla, *Eur. J. Org. Chem.*, 2022, e202200249.
142 S. Munusamy, S. Swaminathan, D. Jothi, V. P. Muralidharan and S. K. Iyer, *RSC Adv.*, 2021, **11**, 15656–15662.
143 Y. Zhao, L. Feng, X. Meng and J. Guan, *Dyes Pigm.*, 2020, **183**, 108713.
144 X. Wen, Q. Wang and Z. Fan, *J. Lumin.*, 2018, **194**, 366–373.
145 Q. Wang, X. Wen and Z. Fan, *J. Photochem. Photobiol., A*, 2018, **358**, 92–99.
146 X. Wen, L. Yan and Z. Fan, *J. Photochem. Photobiol., A*, 2021, **405**, 112969.
147 N. Dey, J. i. Kulhánek, F. Bureš and S. Bhattacharya, *J. Org. Chem.*, 2018, **84**, 1787–1796.
148 N. Dey, J. Kulhanek, F. Bureš and S. Bhattacharya, *J. Org. Chem.*, 2021, **86**, 14663–14671.
149 X. Zhang and D. W. MacMillan, *J. Am. Chem. Soc.*, 2016, **138**, 13862–13865.
150 Z. Zuo, H. Cong, W. Li, J. Choi, G. C. Fu and D. W. MacMillan, *J. Am. Chem. Soc.*, 2016, **138**, 1832–1835.
151 C. K. Prier, D. A. Rankic and D. W. MacMillan, *Chem. Rev.*, 2013, **113**, 5322–5363.
152 V. Srivastava, P. K. Singh and P. P. Singh, *J. Photochem. Photobiol., C*, 2022, 100488.
153 N. A. Romero and D. A. Nicewicz, *Chem. Rev.*, 2016, **116**, 10075–10166.
154 Y. Lee and M. S. Kwon, *Eur. J. Org. Chem.*, 2020, **2020**, 6028–6043.
155 J. Luo and J. Zhang, *ACS Catal.*, 2016, **6**, 873–877.
156 T.-Y. Shang, L.-H. Lu, Z. Cao, Y. Liu, W.-M. He and B. Yu, *Chem. Commun.*, 2019, **55**, 5408–5419.
157 P. P. Singh and V. Srivastava, *Org. Biomol. Chem.*, 2021, **19**, 313–321.
158 Y. Zhao, C. Zhang, K. F. Chin, O. Pytela, G. Wei, H. Liu, F. Bureš and Z. Jiang, *RSC Adv.*, 2014, **4**, 30062–30067.
159 Z. Burešová, V. Jandová, M. Klikar, M. Grygarová and F. Bureš, *Org. Biomol. Chem.*, 2022, **20**, 9378–9384.
160 Z. Hloušková, M. Klikar, O. Pytela, N. Almonasy, A. Růžička, V. Jandová and F. Bureš, *RSC Adv.*, 2019, **9**, 23797–23809.
161 Z. Hloušková, J. Tydlitát, M. Kong, O. Pytela, T. Mikysek, M. Klikar, N. Almonasy, M. Dvořák, Z. Jiang and A. Růžička, *ChemistrySelect*, 2018, **3**, 4262–4270.
162 K. Cao, S. M. Tan, R. Lee, S. Yang, H. Jia, X. Zhao, B. Qiao and Z. Jiang, *J. Am. Chem. Soc.*, 2019, **141**, 5437–5443.
163 G. Wei, C. Zhang, F. Bureš, X. Ye, C.-H. Tan and Z. Jiang, *ACS Catal.*, 2016, **6**, 3708–3712.
164 L. Lin, X. Bai, X. Ye, X. Zhao, C. H. Tan and Z. Jiang, *Angew. Chem.*, 2017, **129**, 14030–14034.
165 B. Qiao, C. Li, X. Zhao, Y. Yin and Z. Jiang, *Chem. Commun.*, 2019, **55**, 7534–7537.
166 C. Zhang, S. Li, F. Bureš, R. Lee, X. Ye and Z. Jiang, *ACS Catal.*, 2016, **6**, 6853–6860.

